# COUPLED VSTOL AIRCRAFT AND SHIP AIRWAKE TURBULENT FLOW SIMULATION MODEL

J.K. Jordan, S.A. Bayyuk, and S.D. Habchi
CFD Research Corporation
215 Wynn Drive, Suite 501
Huntsville, AL 35805

June 2002

FINAL REPORT FOR APRIL 2002 – JUNE 2002
Contract Number: N68335-02-C-3055
CFDRC Report Number: 8408/3

DISTRIBUTION STATEMENT

Approved for public release; distribution is unlimited.

Prepared for

NAVAL AIR WARFARE CENTER- AIRCRAFT DIVISION
ATTN: Susan A. Polsky - Code 4.3.2.1
48110 Shaw Road
Patuxent River, MD 20670

20020625 067

# REPORT DOCUMENTATION PAGE

| | |
|---|---|
| 1a. REPORT SECURITY CLASSIFICATION<br>Unclassified | 1b. RESTRICTIVE MARKINGS |
| 2a. SECURITY CLASSIFICATION AUTHORITY | 3. DISTRIBUTION/AVAILABILITY OF REPORT<br>Approved for public release;<br>Distribution is unlimited. |
| 2b. DECLASSIFICATION/DOWNGRADING SCHEDULE | |
| 4. PERFORMING ORGANIZATION REPORT NUMBER(S)<br>8408/3 | 5. MONITORING ORGANIZATION REPORT NUMBER(S) |
| 6a. NAME OF PERFORMING ORGANIZATION<br>CFD Research Corporation<br>6b. OFFICE SYMBOL *(if applicable)* | 7a. NAME OF MONITORING ORGANIZATION<br>Naval Air Warefare Center-Aircraft Division |
| 6c. ADDRESS *(City, State and ZIP Code)*<br>215 Wynn Drive, Suite 501<br>Huntsville, AL 35805 | 7b. ADDRESS *(City, State and ZIP Code)*<br>48110 Shaw Road<br>Patuxent River, MD 20670 |
| 8a. NAME OF FUNDING/SPONSORING ORGANIZATION<br>8b. OFFICE SYMBOL *(if applicable)* | 9. PROCUREMENT INSTRUMENT IDENTIFICATION NUMBER |
| 8c. ADDRESS *(City, State and ZIP Code)* | 10. SOURCE OF FUNDING NUMBERS<br>PROGRAM ELEMENT NO. / PROJECT NUMBER / TASK NUMBER: 0001AC / WORK UNIT NUMBER |
| 11. TITLE *(include Security Classification)*<br>Coupled VSTOL Aircraft and Ship Airwake Turbulent Flow Simulation Model | |
| 12. PERSONAL AUTHOR(S)<br>J.K. Jordan, S.A. Bayyuk, and S.D. Habchi | |
| 13a. TYPE OF REPORT<br>Final Report | 13b. TIME COVERED<br>FROM April 2002 TO June 2002 |
| 14. DATE OF REPORT *(Year Month Day)*<br>June 2002 | 15. PAGE COUNT<br>63 |
| 16. SUPPLEMENTARY NOTATION | |
| 17. COSATI CODES<br>FIELD / GROUP / SUB GR | 18. SUBJECT TERMS *(Continue on reverse if necessary and identify by block number)*<br>CFD, JSF, Ship Airwake, VSTOL, Overset, Chimera |

19. ABSTRACT *(Continue on reverse if necessary and identify by block number)*

The objective of this SBIR program is to develop an efficient computational tool for the prediction of the complex coupled flow field of a VSTOL aircraft and a ship airwake. The proposed approach couples a hybrid chimera/overset mesh methodology with hybrid advanced flow solver methodology for the VSTOL aircraft and ship air wake flow predictions. This approach utilizes a pressure-based flow solver for the low-speed flow of the ship, and a density-based flow solver for the high-speed flow of the VSTOL aircraft. The focus of this Phase I study was to develop and validate the computational capability to separately predict an aircraft VSTOL flow field and flow over a ship structure. A density-based flow solver, CFD-FASTRAN, using blocked, structured meshes, was validated for VSTOL applications. A pressure-based flow solver, CFD-ACEU, using unstructured Cartesian meshes, was validated for ship airwake applications. To demonstrate the viability of the proposed approach for prediction of the complex, coupled VSTOL aircraft/ship airwake, a simulation of a JSF in hover and a solution for a coupled structured aircraft/Cartesian ship were also obtained.

| | |
|---|---|
| 20. DISTRIBUTION/AVAILABILITY OF ABSTRACT<br>UNCLASSIFIED/UNLIMITED ☒ SAME AS RPT ☐ DTIC USERS ☐ | 21. ABSTRACT SECURITY CLASSIFICATION<br>Unclassified |
| 22a. NAME OF RESPONSIBLE INDIVIDUAL<br>J. Keith Jordan | 22b. TELEPHONE NUMBER *(include area code)*<br>(256) 726-4972<br>22c. OFFICE SYMBOL |

DD FORM 1473, 83 APR EDITION OF 1 JAN 73 IS OBSOLETE

## SUMMARY

The objective of this SBIR program (both Phase I and Phase II) is to develop an efficient computational tool for the prediction of the complex coupled flow field of a VSTOL aircraft and a ship airwake. CFDRC's overall proposed approach couples a hybrid chimera/overset mesh methodology with hybrid advanced flow solver methodology for the VSTOL aircraft and ship air wake flow predictions. This approach utilizes a pressure-based flow solver for the low-speed flow of the ship, and a density-based flow solver for the high-speed flow of the VSTOL aircraft. The focus of the Phase I study was to develop and validate the computational capability to separately predict an aircraft VSTOL flow field and flow over a ship structure. The accomplishments of this Phase I study can be summarized as follows:

- A computational capability that utilizes an existing well-validated density-based flow solver, CFD-FASTRAN, was adapted, validated and demonstrated for VSTOL applications.

- VSTOL in-ground-effect flow field predictions were validated by comparison to test data. The code was applied to several VSTOL simulations using a structured blocked mesh approach and the results compared to test data. The computational predictions agreed well with the data. The capability of modeling the very complex geometry and flow field of a full aircraft was demonstrated by applying a structured overset mesh approach to the X-35B aircraft in VSTOL mode.

- An existing viscous Cartesian grid generator was adapted and utilized to generate viscous grids for a ship. This automatic grid generation capability efficiently generates octree and $2^n$-tree based Cartesian grids with flexibility for grid clustering through the use of sources.

- A computational capability that utilizes an existing arbitrary polyhedral unstructured pressure-based flow solver technology was selected and implemented to model the transient airwake of a large ship. Cartesian grids with viscous spacing were used for the simulations. This flow solver uses advanced high-order numerical schemes and several turbulence models, including a Large Eddy Simulation model.

- The unsteady turbulent air wake flow predictions of the pressure-based flow solver were systematically validated against several problems. Laminar and LES solutions were obtained for the flow over a rib in a channel and showed close agreement with experimental results. The results obtained for the flow over a wind-tunnel model of an LHA class ship matched the corresponding wind-tunnel test results with acceptable accuracy.

- A conceptual approach to couple the flow fields of the ship and VSTOL aircraft was developed. This approach was demonstrated by utilizing an existing computational environment and a chimera/overset grid approach.

The technology development and integration of the various tools will be implemented in Phase II. The flow solvers will be coupled using a seamless approach that utilizes a chimera methodology and a grid adaptation model that will be embedded into a Ship and Aircraft Simulation Model (SASM) that will be developed in Phase II. The SASM model will be based on an existing multi-disciplinary computing environment called MDICE. This computing environment is used to couple different software packages by passing information between the packages. The flow solvers will include high-order advanced numerical schemes for both the density-based and pressure-based solutions, and several turbulence models including Detached Eddy Simulation (DES) turbulence model and several one and two equation turbulence models. With this approach, the user will be able to use any grid topology and construct the ship and aircraft in one mesh system or separately and then combine the meshes. After the mesh system has been obtained, it can be used to obtain high fidelity, time-accurate predictions of the interacting VSTOL flow and the ship air wake. This approach provides flexibility in positioning the aircraft, provides flexibility in mesh construction, allows the re-use of existing meshes, minimizes the time required for a solution, and provides an accurate prediction capability.

## PREFACE

This is the final report for the SBIR Phase I contract entitled "Coupled VSTOL Aircraft and Ship Airwake Turbulent Flow Simulation Model". This project was sponsored by the US Navy, Naval Air Warfare Center- Aircraft Division (NAWC-AD Contract Number N68335-02-C-3055), and performed by researchers at CFD Research Corporation (CFDRC Project Number 8408). The Project Manager was Mr. Sami D. Habchi and the Principal Investigator was Mr. J. Keith Jordan of CFDRC. Ms. Susan A. Polsky was the Navy Technical Monitor.

## ACKNOWLEDGEMENTS

The authors would like to thank Ms. Susan Polsky of the Naval Air Warfare Center/Aircraft Division for her technical assistance. The authors would also like to thank the following CFDRC personnel:

- Dr. Jim Keenan for his work in development of the CFD-FASTRAN flow solver.
- Mr. Rohit Jain for his CFD-FASTRAN technical support.
- Dr. Robert Tramel for his consultation and technical assistance on solution methodology
- Dr. Mark Underwood and Dr. Vijayan Parthasarthy for their assistance in the coupled ship/aircraft demonstration.
- Dr. Wei Yuan for his assistance and his work in the development of the CFD-VisCART Cartesian mesh generation software.
- Mr. Keith McDaniel for his assistance in the LES problem setup.

## TABLE OF CONTENTS

## LIST OF FIGURES

## LIST OF FIGURES *(cont.)*

# 1. INTRODUCTION

## 1.1 Background

Fixed-wing VSTOL aircraft encounter unique challenges during shipboard Dynamic Interface (DI) operations. As a VSTOL aircraft approaches a ship, the flow from the propulsion system interacts with the unsteady flow passing over the deck, causing an unstable flow field in which the pilot must maneuver. This unsteady environment increases the difficulty of trimming the aircraft and requires the pilot to make continuous changes in control settings, drastically increasing the pilot workload. The problem can be compounded in the presence of high winds and rough seas. As the ship motion and the turbulence levels of the flow over the deck increase, so does the danger to the pilot, aircraft, and deck crew. In many conditions, the ship motion and deck turbulence make it impossible to land VSTOL aircraft at all. Obviously, defining the envelopes in which a VSTOL aircraft may safely land on a ship is of great concern to the U.S. Navy.

The primary method of determining the safe operating envelopes, also known as wind-over-deck (WOD) envelopes, is by full-scale flight testing. While providing much needed information, these trials are quite costly because they require the dedicated use of a ship, aircraft, and the personnel to support the test. Small-scale wind tunnel tests can also be used to obtain ship air wake information. While less expensive than the full-scale flight test, wind tunnel tests are still costly and have measurement and scaling issues that must be dealt with. The flow features above the deck are critical in the prediction of the handling characteristics of a landing VSTOL aircraft. However, obtaining off-body data in the wind tunnel is often difficult and adds to the expense of the test. Model scaling is an issue because the scale factors required for building reasonably sized ship wind tunnel models are generally in the 1/100th range. Unfortunately, at this scale, the available wind tunnel hardware is not able create a flow to match the full scale Reynolds number. Therefore, the small-scale instabilities may be difficult to scale to full-scale values or they may be inadequately modeled.

It is for the aforementioned reasons that a computational prediction capability is so attractive. Computational Fluid Dynamics offers a safe, relatively inexpensive addition to flight and wind tunnel testing. CFD has been used in the aerospace community for a number of years, and numerous computational investigations have taken place in the last several years to predict ship air wakes (Refs. 1-6).

### 1.1.1 Physical Phenomena

Fixed-wing VSTOL aircraft generate vertical lift using multiple downward-directed jets, and the flow patterns underneath them share some common flow phenomena. When a vertically directed jet contacts the ground, it spreads in a flat, circular pattern. In general, the pattern is a high speed, high temperature flow that can be dangerous to nearby ground personnel. In the case of multiple impinging jets, the spreading jets contact each other, causing the flow to be redirected upward toward the aircraft. In some cases, the resulting fountain is a high temperature upward flow that contacts the aircraft skin. It is possible that the temperature at the impingement point may be high enough to damage components at that location. Another phenomenon of interest is referred to as "suckdown". Turbulent mixing entrains surrounding air into the jet flow. This

entrainment accelerates the ambient air around the jet, lowering the pressure underneath the wing and fuselage resulting in forces that counteract some of the lift generated by the jets. Hot gas ingestion is also a concern for VSTOL aircraft. Hot gas ingestion can occur during vertical landing when the jet engine inlet draws in re-directed hot gas from the engine. As the temperature of the gas ingested by the engine rises, the performance of the engine drops. The loss of engine power coupled with the suckdown effect is obviously a serious concern during landing.

As stated previously, the flow over the deck of a large ship is characterized by very large regions of low-speed, time-varying, separated flow. As the air passes over the deck, vortices are generated by the corners of the components of the ship, causing an unstable flow field in which the pilot must land. This unsteady environment causes fluctuations in the aircraft loads and may drastically increase the difficulty of controlling the aircraft. These massively separated regions will change size, shape, and location as the wind-over-deck angle changes. The flow field and landing will be further affected by the motion of the ship in rough seas. For these reasons, landing a VSTOL aircraft on a ship can be a very difficult enterprise, and in many conditions not possible at all.

### 1.1.2 Computational Challenges

CFD simulations begin with modeling the flow volume with a computational mesh. There are two basic approaches to mesh generation- structured meshes and unstructured meshes. Both approaches have several types of meshes that can be constructed. Unstructured meshes are typically tetrahedral or cartesian, with several methods used to model the boundary layer region. Structured meshes can be blocked, patched, or overset. Each type of mesh has its own advantages and disadvantages. In general, unstructured meshes typically require less labor than structured meshes, but the memory requirements are higher, proper resolution of the boundary layer region may be problematic, and a high quality mesh with low skewness may be difficult to obtain. Structured meshes typically result in better mesh quality and require less memory, but require more labor, and can be extremely difficult to generate for very complex bodies. Which type of mesh to be used is determined by the flow phenomena, geometry, and user preferences. In the case of DI predictions and WOD envelopes, the construction of the grid systems for all the required positions of the aircraft on or near the ship, as well as for different types of ships and aircraft will be very labor intensive.

The next component of the computational prediction process is the flow solver. Any computational solver developed for the DI problem must accurately predict time-accurate, highly turbulent, mixed high- and low-speed flow. Many density-based codes, which are typically used for high-speed flows, must use a pre-conditioner or Mach scaling (Ref. 1) to enhance stability and accuracy when applied to the low-speed flow over a ship. Most pressure based codes, used for low speed flows, are unable to model the high-speed compressible flows that exit from the aircraft nozzles. Recent studies show that the dissipation introduced by turbulence models will dampen the unsteadiness of time-varying flows and that the Large Eddy Simulation (LES) or the emerging Detached Eddy Simulation (DES) technology, may be required for accuracy (Ref. 7). Additionally, time accurate numerical simulations of the ship air wake and the VSTOL aircraft flow field is currently computationally intensive and laborious. Large computational grids, perhaps on the order of several million cells, may be needed to resolve the complex geometry of

the ship and aircraft, and to capture the complex flow structures. It may be required to model several seconds of real time to fully resolve the flow phenomena, requiring tens of thousands of iterations of the solver, and from hundreds to thousands of CPU hours.

Obviously, then, there are many things to consider when designing a methodology to be used in simulations of the DI problem.

## 1.2 Phase I Objectives

The Phase I work is a first step toward the coupled ship/aircraft prediction capability required for Phase II. CFDRC's specific objectives for the Phase I work were to:

1. Develop a computational capability within the CFD-FASTRAN flow solver for predicting VSTOL-in-ground-effects flow fields, including the addition of a $2^{nd}$ order time-marching scheme.

2. Systematically validate VSTOL in-ground-effect flow field predictions by comparing the CFD predictions to test data.

3. Develop a computational approach to accurately and efficiently model the transient airwake of a large ship.

4. Validate the air wake predictions by comparing to wind tunnel data.

5. Develop a conceptual approach for coupling ship airwake and VSTOL aircraft flow fields.

6. Document the results of the work in a formal report.

## 1.3 Summary of Phase I Accomplishments

The Phase I accomplishments can be summarized as follows:

1. A computational capability within the CFD-FASTRAN flow solver for predicting VSTOL-in-ground-effects flow fields was developed. A boundary condition to model the aircraft propulsion system was completed and incorporated into the code. A $2^{nd}$ order time-marching scheme was incorporated.

2. VSTOL in-ground-effect flow field predictions were validated by comparison to test data. The CFD-FASTRAN code was applied to several VSTOL simulations using a structured blocked mesh approach and the results compared to test data. The computational predictions agreed well with the data. The capability of modeling the very complex geometry and flow field of a full aircraft in VSTOL mode was demonstrated using a structured, overset mesh approach. A solution was obtained on an X-35B geometry, complete with open doors, extended gear, and flowing inlets and exhausts. While no data was available for comparison, the results are consistent with engineering judgments.

3. A computational approach to model the transient airwake of a large ship was selected. This approach utilizes an adaptive viscous Cartesian grid generation methodology for generating the computational grid, and a pressure-based arbitrary polyhedral unstructured flow solver for flow predictions. An existing viscous Cartesian grid generation tool, called CFD-VisCART, was adapted for ship airwake grid generation.

4. The air wake predictions were validated by comparison to wind tunnel data. Validations were first performed on a rib in a channel. Laminar and LES flow models were utilized in this validation study, with the LES model yielding the best results.

5. Predictions were performed for the LHA ship at wind tunnel conditions. Two Cartesian grids with different resolutions were used. The results compared well to test data.

6. A conceptual approach for coupling ship airwake and VSTOL aircraft flow fields was developed. The approach couples a hybrid chimera/overset mesh methodology with advanced parallelized pressure-based and density-based flow solvers. The proposed approach supports all types of grid topologies for both the aircraft and ship. The pressure-based flow solver is used for solving the low-speed flow of the ship, while the density-based flow solver is used for solving the high-speed VSTOL aircraft flow field. The two solutions are coupled using an automated unstructured chimera methodology integrated in an existing multi-disciplinary computing environment.

7. The results of the work, conclusions, and recommendations for Phase II are documented in this report.

The accomplishments of Phase I show the feasibility of the proposed Phase II work. The proposed methodology enhances and extends current computational tools so that the coupled VSTOL/ship airwake flow field can be accurately and efficiently predicted. The VSTOL computational capability is proven, while the shortcomings and associated solutions for the ship airwake computational capability have been identified.

## 2. COMPUTATIONAL APPROACH

The overall technical approach to be developed, implemented and validated in both Phase I and Phase II has been outlined above. Most of the development for this technology will be implemented in Phase II. The computational technique proposed in this work relies on coupling together two different flow solvers, the density-based CFD-FASTRAN solver and the pressure-based CFD-ACEU solver, through the Ship and Aircraft Simulation Model that utilizes a generalized unstructured chimera module and a grid adaptation module. The integrated package will provide great flexibility in the computation of coupled solutions containing a ship and one or more VSTOL aircraft. Most of the Phase I work was directed at testing, establishing, and validating the relevant capabilities of the two different flow solvers, CFD-FASTRAN and CFD-ACEU, and the CFD-VisCART grid-generation and adaptation tool. Work was also directed toward ensuring that these individual components can be used together effectively. The basic capabilities of these software tools, along with modifications made under this Phase I, effort are discussed below.

### 2.1 CFD-FASTRAN Flow Solver

The density-based flow solver, CFD-FASTRAN (Ref. 8), was used as the platform for solving the flow field in the VSTOL aircraft grid(s). The salient features of the current version of the CFD-FASTRAN flow solver include:

- Density based finite-volume formulation.
- Euler or Navier Stokes equations for 2D, 3D and Axi-Symmmetric flows.
- Multi-zone structured, general unstructured and hybrid grid capability.
- An automated chimera/overset technology for structured grids.
- Baldwin-Lomax, k-ε, k-ω and Spalart-Allmaras turbulence models for structured grids.
- k-ε, Spalart-Almaras, k-ω and Menter-SST turbulence models for unstructured grids.
- Roe or Van Leer upwind spatial differencing, and Min-Mod, Van Leer, Osher-C, and the MUSCL flux limiting scheme for structured meshes
- Roe scheme with Venkat, Barth, or MUSCL limiters for unstructured meshes.
- A fully coupled 6-DOF model for body motion.
- Generalized finite rate chemistry and thermal non-equilibrium for structured grids.
- Explicit and implicit time integration.
- An easy-to-use GUI interface for construction of the input deck.

The CFD-FASTRAN multi-block structured flow solver was utilized for solving the flow field of the VSTOL aircraft. The CFD-FASTRAN inflow/outflow boundary condition, which employs a mix of total pressure and fixed mass boundary condition was adapted to model the nozzle inlet flow from the aircraft.

Also, the second-order Crank-Nicholson (C-N) Method time integration scheme was incorporated into the polyhedral unstructured flow solver modules in CFD-FASTRAN. The C-N Method is considered to be unconditionally stable and provides second order accuracy in time. This scheme was added to the unstructured solver for ship airwake predictions.

## 2.2 CFD-ACEU Pressure-Based Flow Solver

The pressure-based flow solver, CFD-ACEU (Ref. 9), was used as the platform for solving the flow field in the ship grid. CFD-ACEU was benchmarked and selected for this application because of its suitability for the low speed flow, the availability of a LES model and the validation predictions made for the LHA configuration. The salient and relevant features of the current version of the CFD-ACEU flow solver include:

- A collocated, fully implicit and strongly conservative finite volume formulation;
- Two- and three-dimensional Navier-Stokes equations models for incompressible and compressible flows;
- Pressure-based solution algorithms including SIMPLE and a variant of SIMPLEC;
- Single and many-to-one multi-domain grid topology;
- Arbitrary grid matching at domain interfaces;
- Structured and arbitrary (unstructured) cell mesh capability;
- Parallel processing capability;
- Upwind, central (with damping), second order upwind, and Osher-Chakravarthy differencing schemes;
- Standard, RNG, and low Reynolds number turbulence models
- Large Eddy Simulation (LES) turbulence model with several sub-grid models

**LES Turbulence Model:** CFD-ACEU employs a Large Eddy Simulation model that has been developed during the last several years under funding from the Air Force and Department of Energy. The CFD-ACEU LES model supports 3D unstructured, time-accurate, parallel, compressible simulations with $2^{nd}$-order spatial and temporal accuracy. Several subgrid models are employed in the solver as discussed below.

**Subgrid Turbulence Models:** Several subgrid turbulence models have been implemented in the CFD-ACEU code. These subgrid models include the original eddy viscosity based model (Ref. 10), a dynamic model that locally computes the Smagorinsky constant based on a test filter (Ref. 11), and a recently developed localized dynamic subgrid kinetic energy model (LDKM) (Ref. 12). The more advanced LDKM model can utilize coarser grids compared to other LES model approaches, does not assume equilibrium between production and dissipation and provides subgrid turbulence information for the Linear Eddy subgrid chemistry model. This dynamic model requires test filters to compute model coefficients and for an unstructured grid, all neighboring cells contribute to the test filter.

**LES Predictions:** CFD-ACEU LES capabilities and the importance of the subgrid models were recently demonstrated under a separate project on a 3D unsteady reacting back-step flow problem. Figure 2.1 shows a snapshot in time of unsteady RANS and LES simulations of the velocity isosurface for non-reacting conditions. Unsteady RANS is too dissipative and does not allow the hydrodynamic instability to develop. Figure 2.2 shows the predicted (LES) and measured instantaneous Schlieren image for the reacting flow. The predictions with a laminar chemistry assumption do not account for the effects of subgrid turbulent strain on the reaction and thus do not allow the vortex roll-up and mixing to occur. The Linear Eddy Mixing (LEM)

subgrid chemistry model was needed to resolve the effects of mixing and reaction down to the molecular level.

a. Unsteady RANS

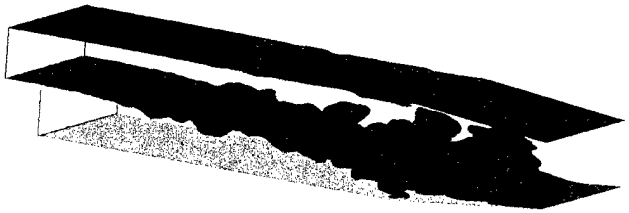

b. LES

*Figure 2.1. Predicted Instantaneous Velocity Isosurface of Turbulent Flow Over a Backstep Using Unsteady RANS and LES*

LES with Laminar Chemistry

LES with Linear Eddy Mixing Model

Measured Schlieren Image

*Figure 2.2. Predicted and Measured Schlieren Image of Turbulent Reacting Flow Over a Backstep*

## 2.3 CFD-GEOM Mesh Generation Software

CFD-GEOM (Ref. 13) was used for any necessary CAD geometry manipulations and to construct all the blocked and overset structured meshes used in this work. CFD-GEOM is an interactive CAD type geometry creation and grid generation tool for structured, unstructured and hybrid grids. Features of CFD-GEOM include:

- Easy-to-Learn, easy-to-use Graphical User Interface with highly intuitive point & click operation.
- Compatibility with IGES formats from other major CAD packages.
- Extensive library of NURBS based geometry creation tools.
- Extensive geometry, topology, and mesh manipulation capabilities with automatic, efficient update of the entire database.
- Automatic and efficient 2D/3D unstructured tetrahedral mesh generation, with interactive mesh clustering control.
- 3D hybrid unstructured/Structured mesh capability for boundary layer resolution.

## 2.4 CFD-VisCART Cartesian Mesh Generation Software

CFD-VisCART (Ref. 14) is CFDRC's automated, 3D, viscous cartesian grid generation tool that was used to generate the mesh for the ship airwake validation work. This technology was developed under a separate Navy SBIR Phase I and Phase II programs for automatic viscous

Cartesian grid generation for aircraft and other complex geometries. It has both an octree and 2n-tree data structure capability. These data structures control the manner in which the flow domain is discretized. With an octree data structure, any cell that is divided to resolve a flow phenomena or geometric entity is divided into eight equal cells. This type of cell refinement is referred to as isotropic refinement. With a $2^n$ –tree data structure, a cell can be divided into two, four or eight cells, see Figure 2.3. This process is referred to as anisotropic refinement, and can significantly reduce the number of cells required to define the flow domain. A cartesian mesh created using anisotropic refinement is very efficient, usually resolving a given flow domain with less cells than would be possible with a tetrathedral mesh. Features of CFD-VisCART include:

- $2^n$ –tree or Octree data structures.
- Point, line, curve, plane, surface, and box sources for control of the local mesh density.
- A viscous layer capability
- Automated and manual tools that can be used to improve grid quality.
- A solution- and source-based adaptation tool for mesh refinement.

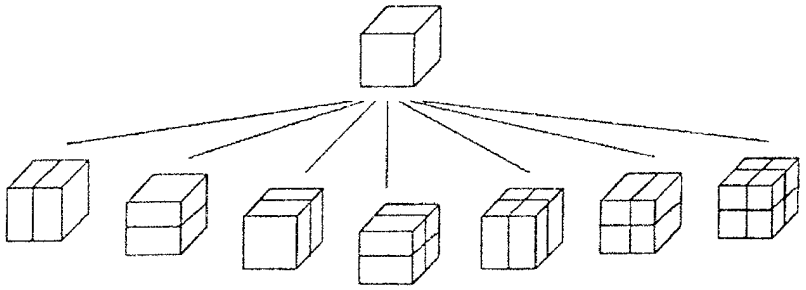

*Figure 2.3. Cell Subdivision of the Cartesian Cell Using Anisotropic Refinement*

Many improvements were made to CFD-VisCART in Phase I. New capabilities for mesh adaptation, specifying mesh density, evaluating cell skewness, identifying negative cell volumes, and repairing of poor quality cells were added. The robustness and stability of the code were also improved.

## 3. VSTOL VALIDATIONS AND DEMONSTRATION

### 3.1 Exact Solution for 2D Impingement (Hiemenz Flow) and Axisymmetric Impingement

Two simple validation cases were found in Reference 15. Exact solutions of the Navier-Stokes equation exist for a low speed, axisymmetric or 2D impingement normal to a surface. These solutions predict the boundary layer profile of the flow across the surface and were used to validate the ability of the CFD-FASTRAN code to model impingement flow at low speed. Both the 2D and axisymmetric cases were run. Plots of non-dimensionalized tangential velocity versus dimensionalized boundary layer thickness, $\eta = \sqrt{(a/\nu)} * h$, are presented in Figure 3.1, where a= -V/h in the linear region of the boundary layer profile, $\nu$ is the kinematic viscosity, and h is the normal distance above the wall. The value of a was determined graphically. The variable u/U is the ratio of the outward velocity in the boundary layer to the velocity at the edge of the boundary layer. The calculations were both run with a 101x101 two dimensional or axisymmetric mesh. As can be seen in the plots, the computational predictions for both cases match the exact Navier-Stokes solution extremely well.

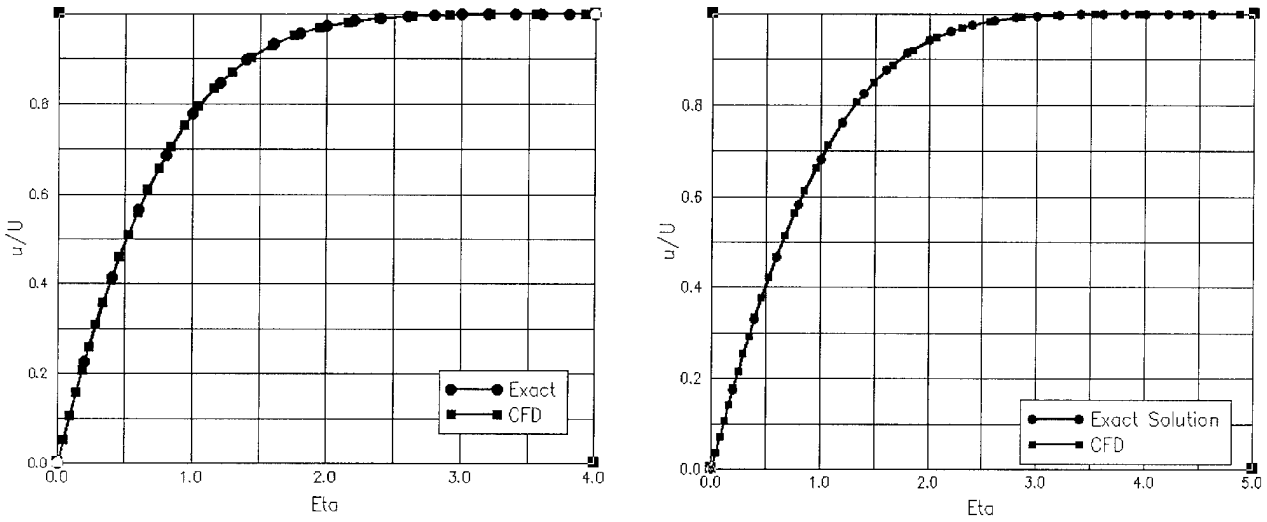


a. 2D Impingement

b. Axisymmetric Impingement

*Figure 3.1. Exact Solution for 2D and Axisymmetric Impingement*

### 3.2 Single Jet Validation

Test data from 20 was a more complicated validation of the VSTOL capabilities of the CFD-FASTRAN flow solver. Reference 16 documents suckdown data from test using circular plates with a jet through the center in stagnant air. The geometry chosen for the validation case is a 20 inch diameter flat plate with a ASME long-radius nozzle, as shown in Figure 3.2. The geometry and flow of the nozzle was modeled in the simulation, as opposed to a jet boundary condition on the plate surface. The NPR chosen was 4.0. Because the plate and nozzle were

circular, a 2D axi-symmetric mesh was used. To begin the work, several solutions were obtained to determine the required mesh size, to determine whether a steady flow model was adequate, and to determine an appropriate turbulence model. It was determined that the mesh system shown in Figure 3.3 was adequate. The system was comprised of approximately 17,000 nodes in four zones. It was also determined that a time-accurate simulation provided better convergence, even though the time variance in the solution eventually disappeared.

The test data reports values for $h/(D - d_e)$ and $(L-L_{inf})/T$, where h is the distance between the bottom of the plate and the ground plane, D is the plate diameter, $d_e$ is the jet exit diameter, L is the lift force generated on the plate, $L_{inf}$ is the lift force generated on the plate out of ground effect, and T is the thrust generated by the nozzle. The values for $(L - L_{inf})$ were obtained by subtracting the plate lift determined from a solution at $h/(D - d_e) = 8$ from the other solutions. Contour plots of Mach Number are included in Figure 3.4, and a comparison of the CFD suckdown predictions to the test data is presented in Figure 3.5. As can be seen from the plot, the predictions obtained using the k-ε turbulence model provide slightly superior results to those obtained with the SST model. Additionally, because no wall function implementation of the SST model was available, the k-ε solutions required less CPU time than the SST solutions. Based on these results, all subsequent VSTOL solutions used the k-ε turbulence model.

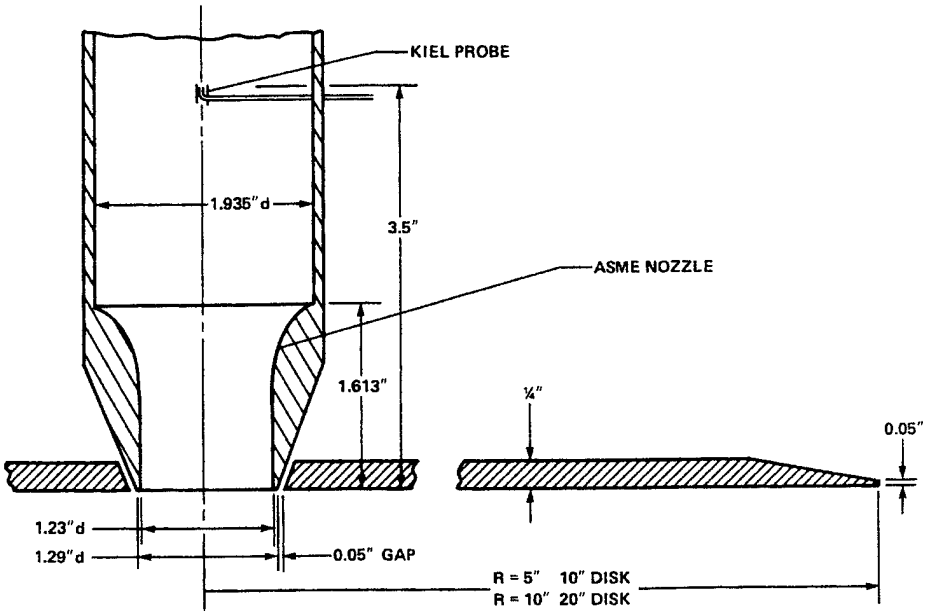


*Figure 3.2. Geometry of the Single-Jet Validation Case, from Reference 16*

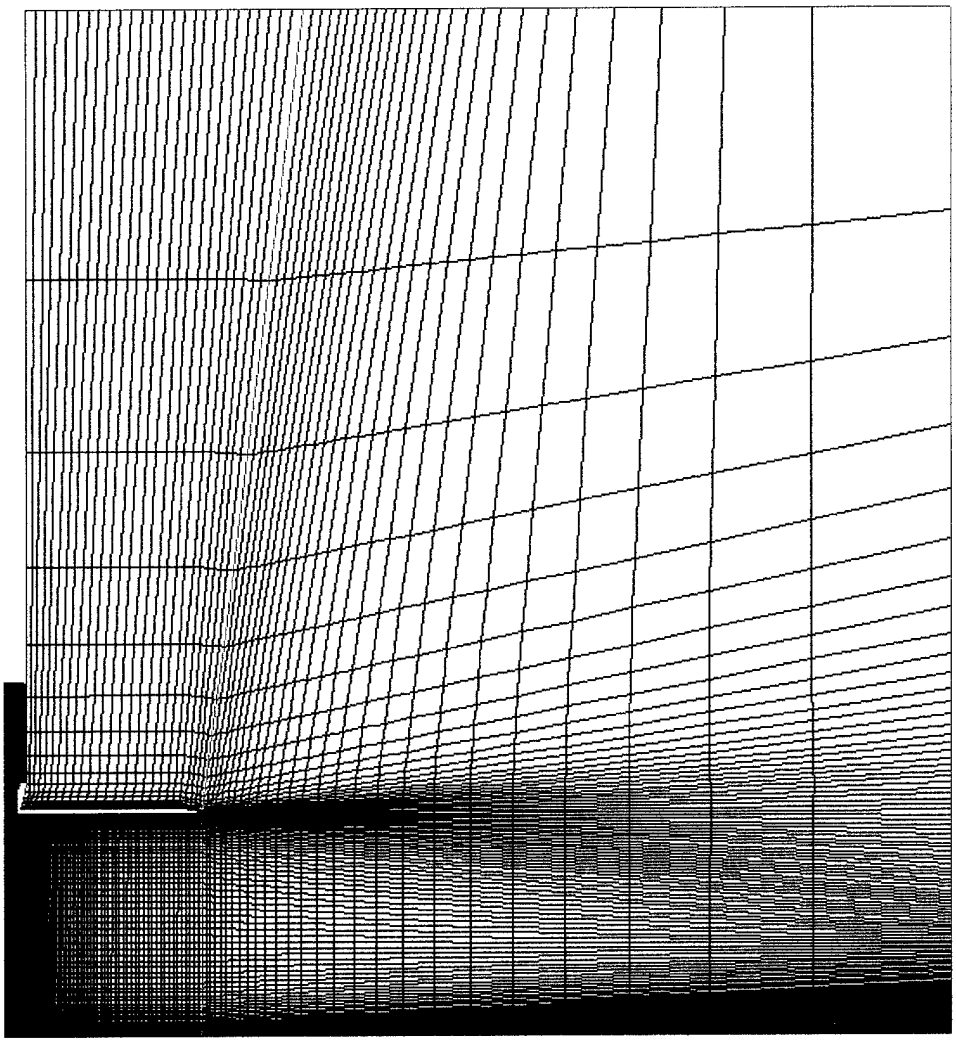

*Figure 3.3. Mesh System for the Single-Jet Validation Case*

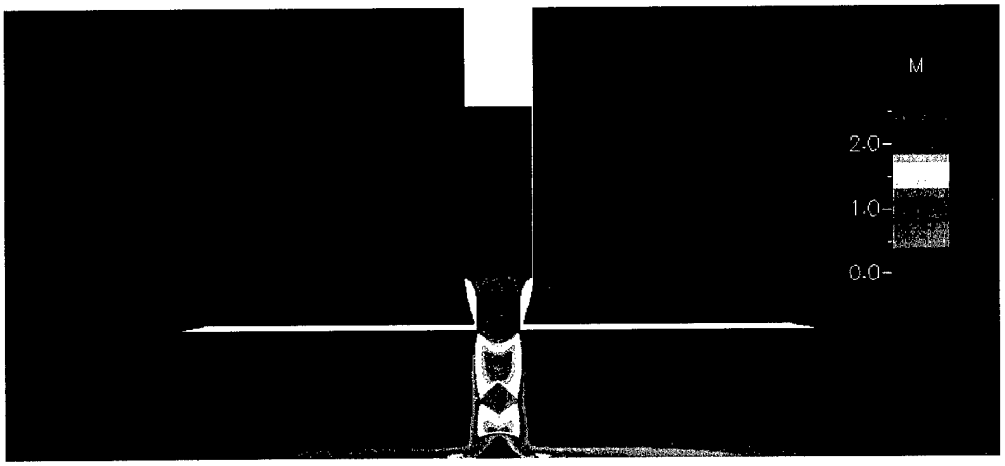


a. $h/(D-d_e) = 0.2$

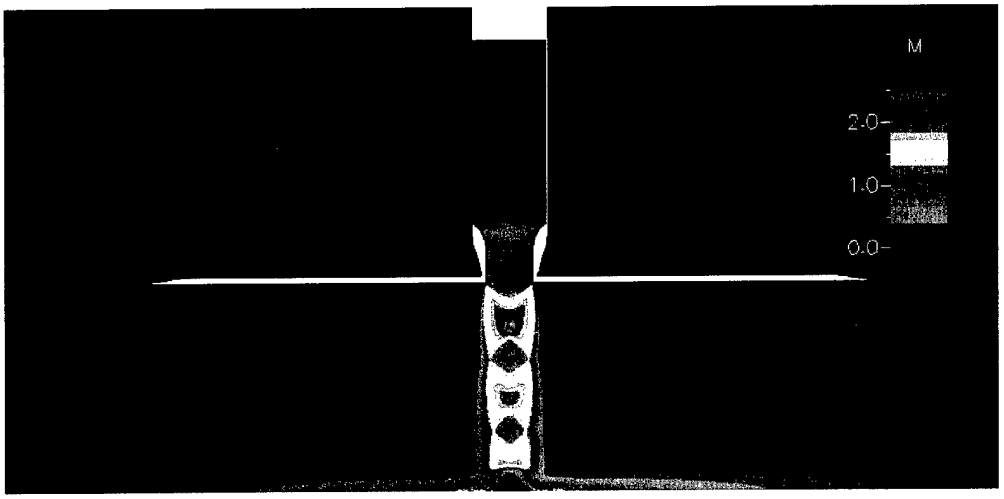


b. $h/(D-d_e) = 0.3$

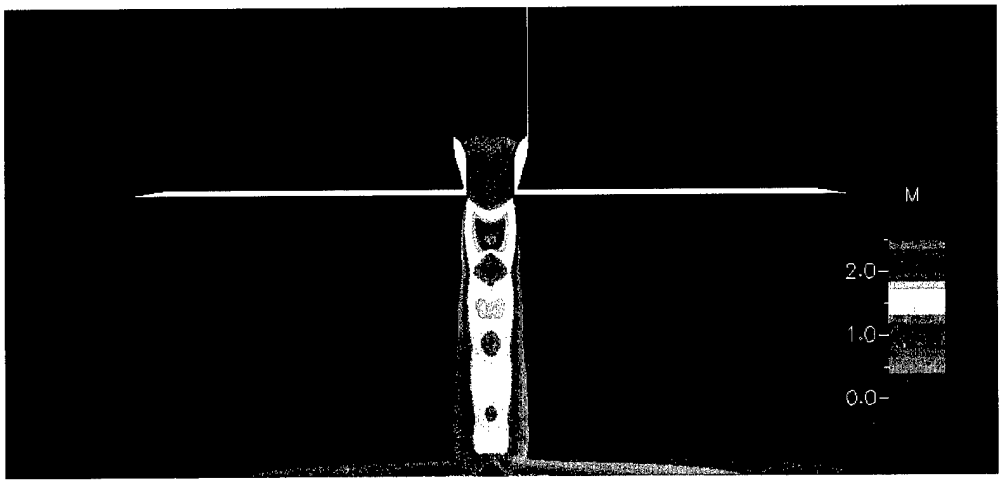


c. $h/(D-d_e) = 0.4$

*Figure 3.4. Single-Jet Validation Case Mach Contour Plots*

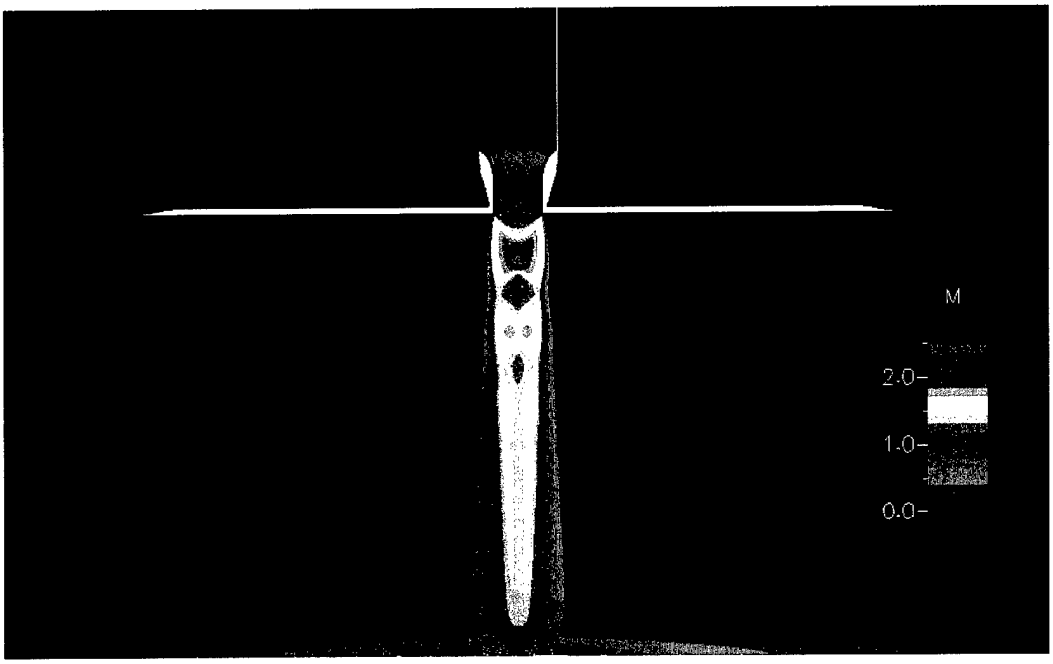


d. h/(D-de) = 0.6

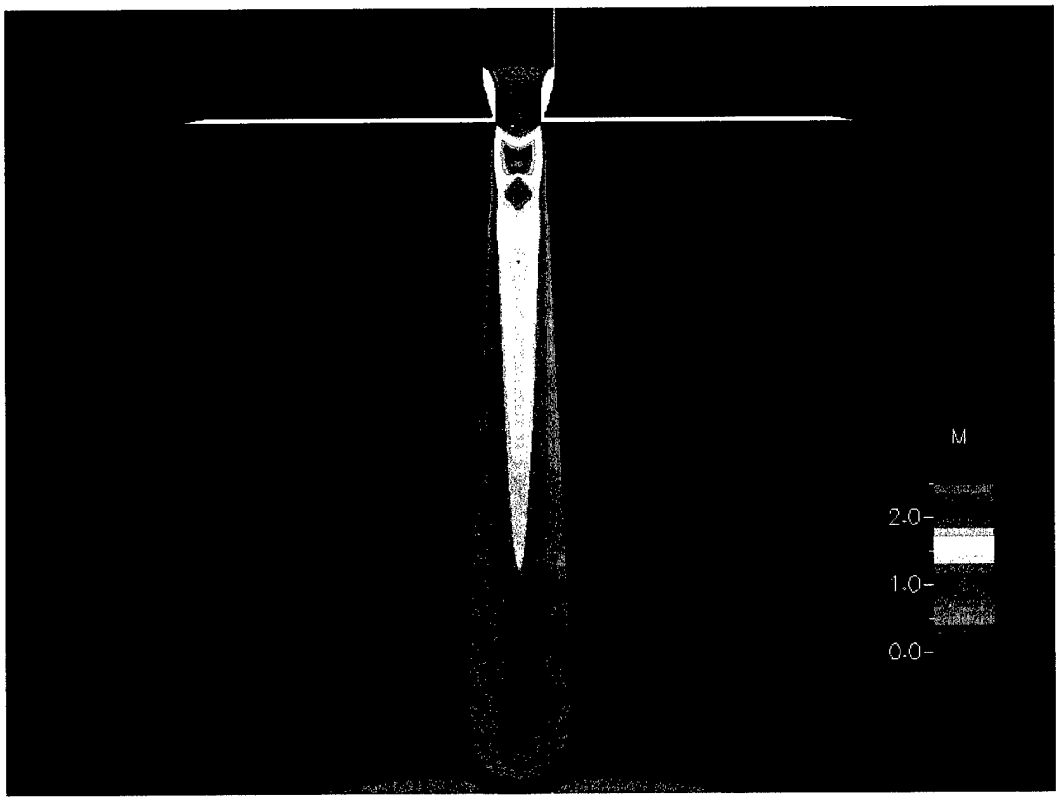


e. $h/(D-d_e) = 1.0$

*Figure 3.4. Single-Jet Validation Case Mach Contour Plots (cont.)*

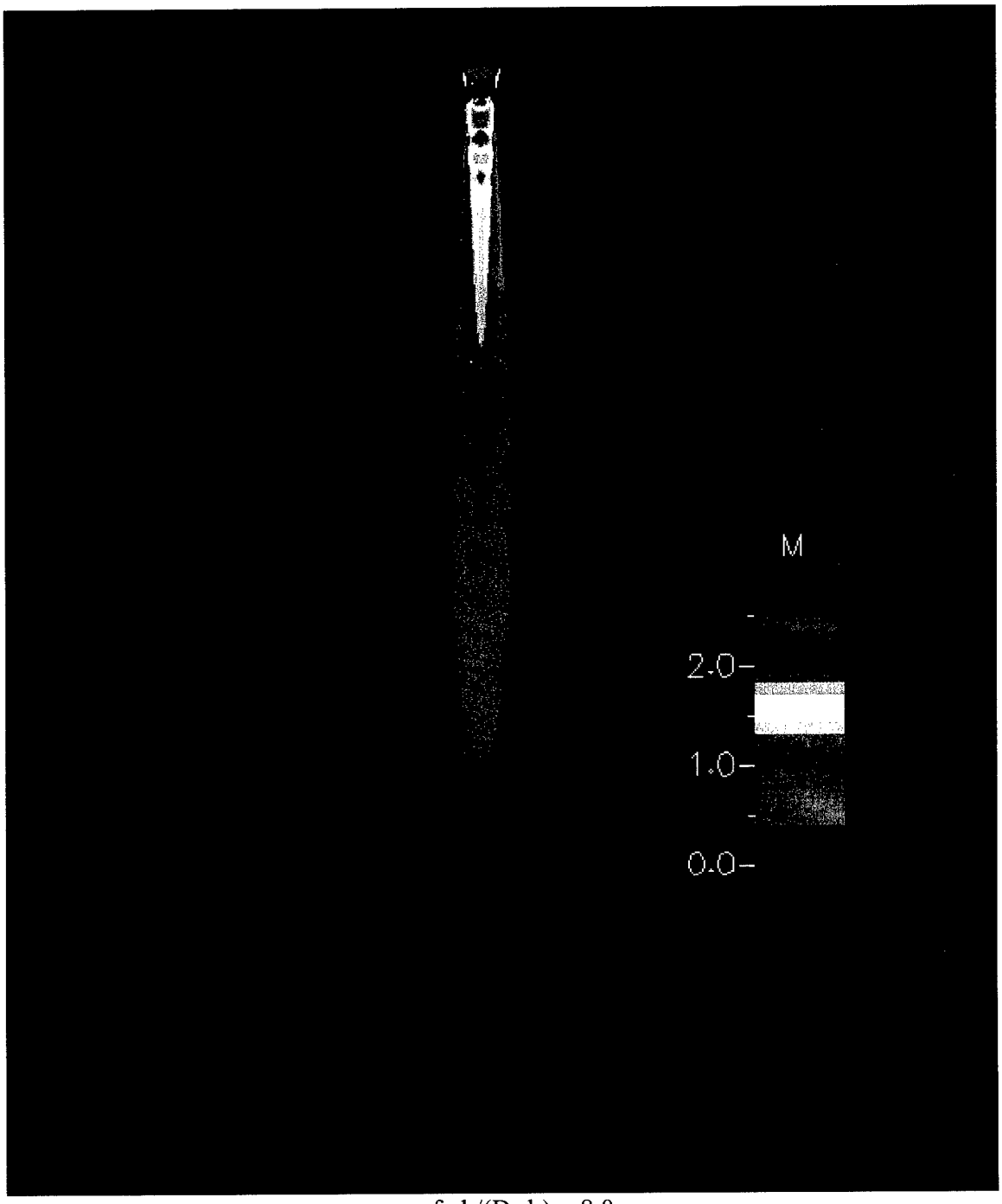


f. $h/(D-d_e) = 8.0$

*Figure 3.4. Single-Jet Validation Case Mach Contour Plots (concluded)*

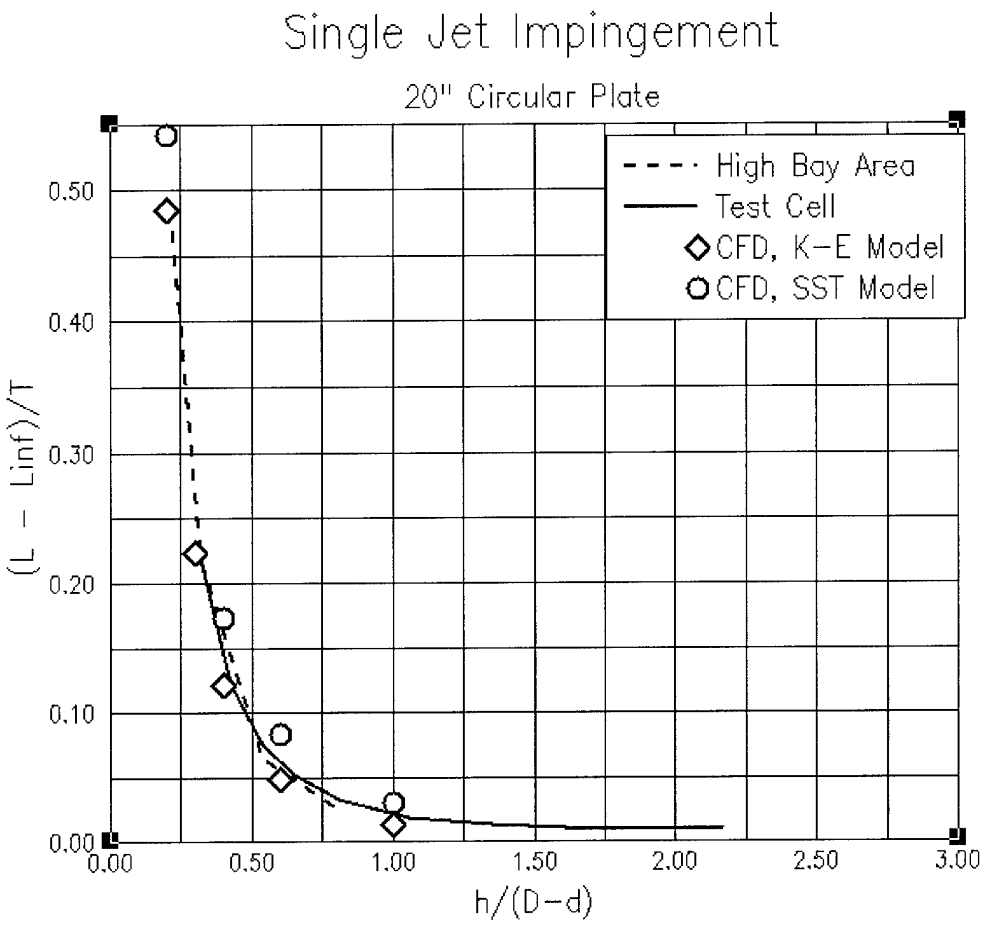


*Figure 3.5. Comparison of Single-Jet CFD Predictions to Test Data*

## 3.3 Twin Jet Validation

Test data from Reference 17 was used to further validate the VSTOL capabilities of the flow solver. Reference 17 documents suckdown and pressure data from a series of tests using various geometries with twin jets in stagnant air. In this validation case, the pressure data was used to determine whether the CFD-FASTRAN solver would be able to predict the fountain created by twin jets. For the chosen validation case, NPR = 4.0 for both jets and the distance between the plate and the ground plane was 0.0741 m, which corresponds to $h/D_e$=1.72 in the test. The geometry consisted of a 12"x8" rectangular plate with a forward and aft jet both mounted along the long axis of the rectangle, and is referred to as Configuration 2C-8-0-12/8 in the test report. A sketch of the plate and nozzle geometry is included in Figure 3.6.

Because the plate was rectangular, only a single plane of symmetry could be used, which greatly increased the size of the mesh as compared to the single-jet validation case. The distribution and number of points were based on the grid study performed for the single-jet validation. A sketch of the mesh system is included in Figure 3.7. This mesh system included 24 blocked zones with a total of approximately 1.8 million nodes. While the test data does include suckdown data, the

time required to obtain a solution on this larger mesh precluded multiple CFD predictions for suckdown. A plot of Mach Number contours at the symmetry plane is presented in Figure 3.8, and a plot of velocity vectors at the symmetry plane is included in Figure 3.9. A comparison of the CFD and test data for Cp on the bottom of the plate is presented in Figure 3.10, where

$$Cp=(P-P_{inf})/q_{jet},$$

$$q_{jet} = 254.431 \text{ KPa, and } P_{inf} = 101.325 \text{ KPa.}$$

In all of the figures, the fountain generated by the interaction of the jets is easily identified. Overall, the agreement between the CFD and the test data is good, but with the CFD not accurately capturing the pressure peaks at the fountain. It is possible that the k-ε turbulence model is overly smoothing the solution and that a DES simulation is more appropriate. Information to fully explain the discrepancy is unavailable. It is interesting to note that at Y=1.5 and 3.0, the test data shows asymmetric results, while the CFD does not. Since the geometry is symmetric about X and the jets have the same NPR, it would be expected that the pressure distribution would also be symmetric.

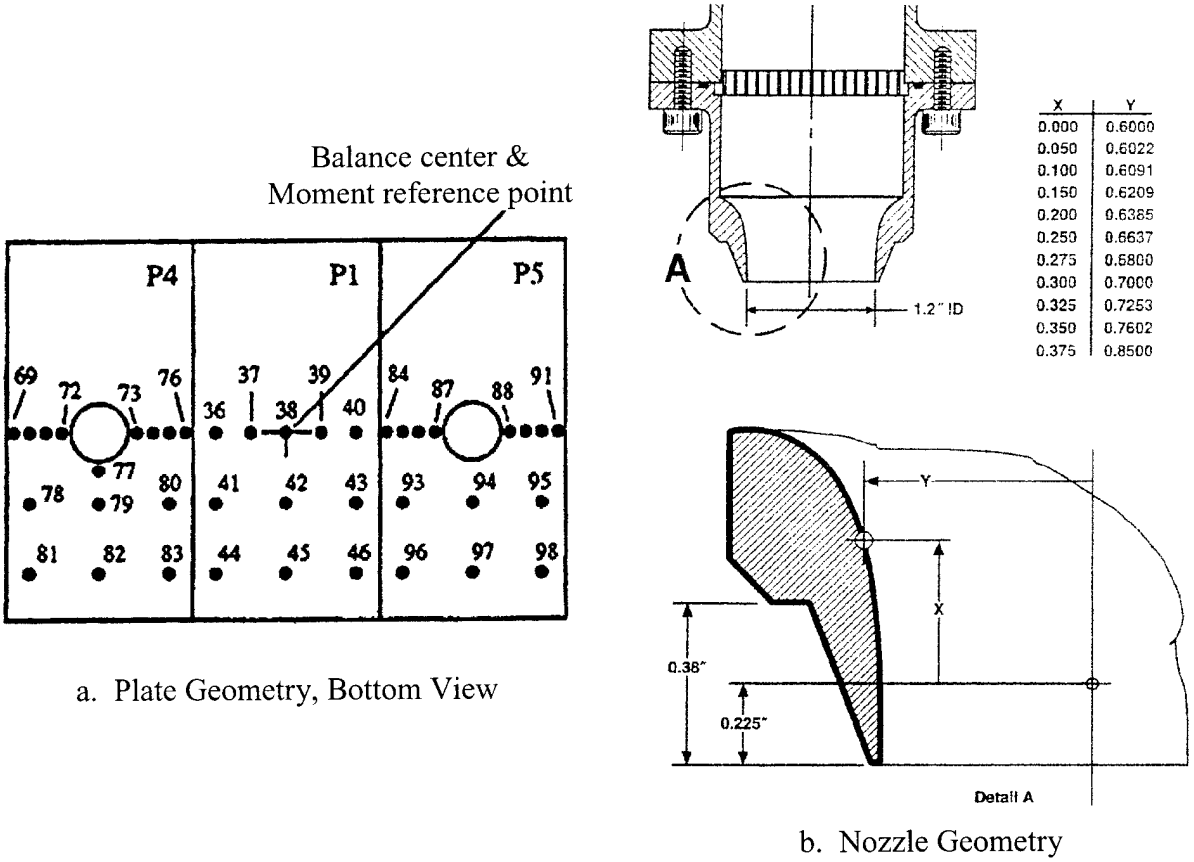


a. Plate Geometry, Bottom View

b. Nozzle Geometry

*Figure 3.6. Geometry of Twin-Jet Validation Case, Configuration 2C-8-0-12/8 from Reference 17*

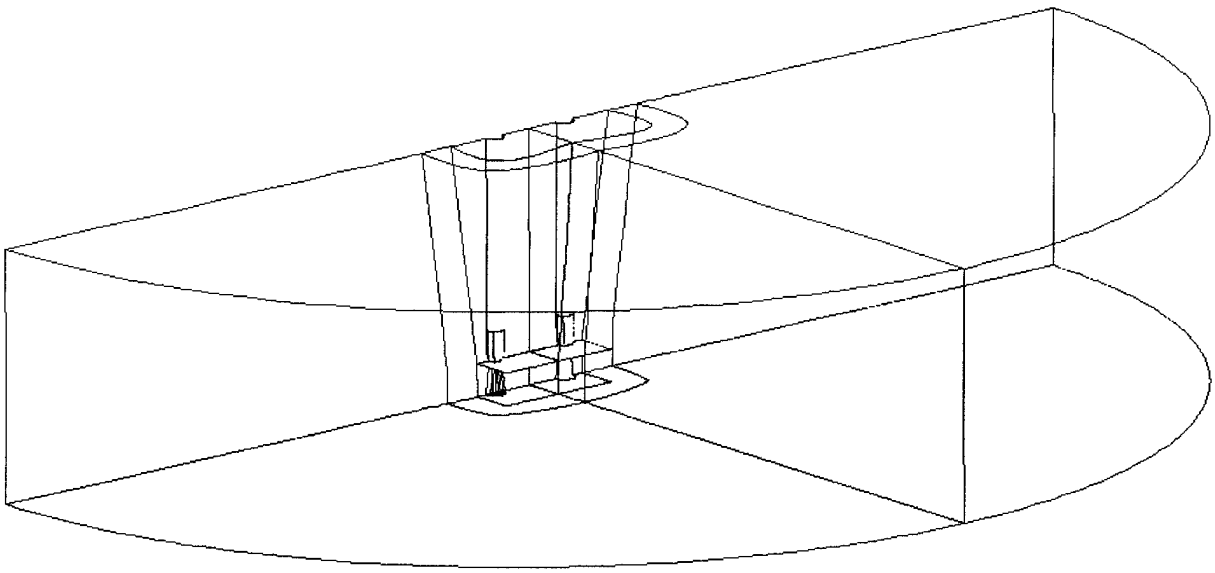

a. Overall Domain

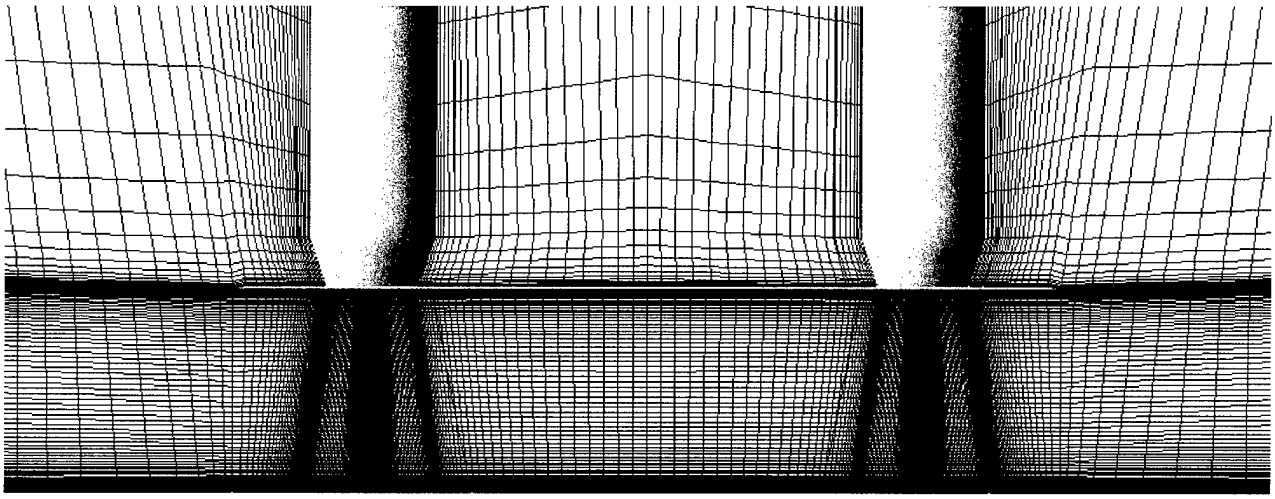

b. Mesh Symmetry Plane Detail

*Figure 3.7. Mesh System for the Twin-Jet Validation Case*

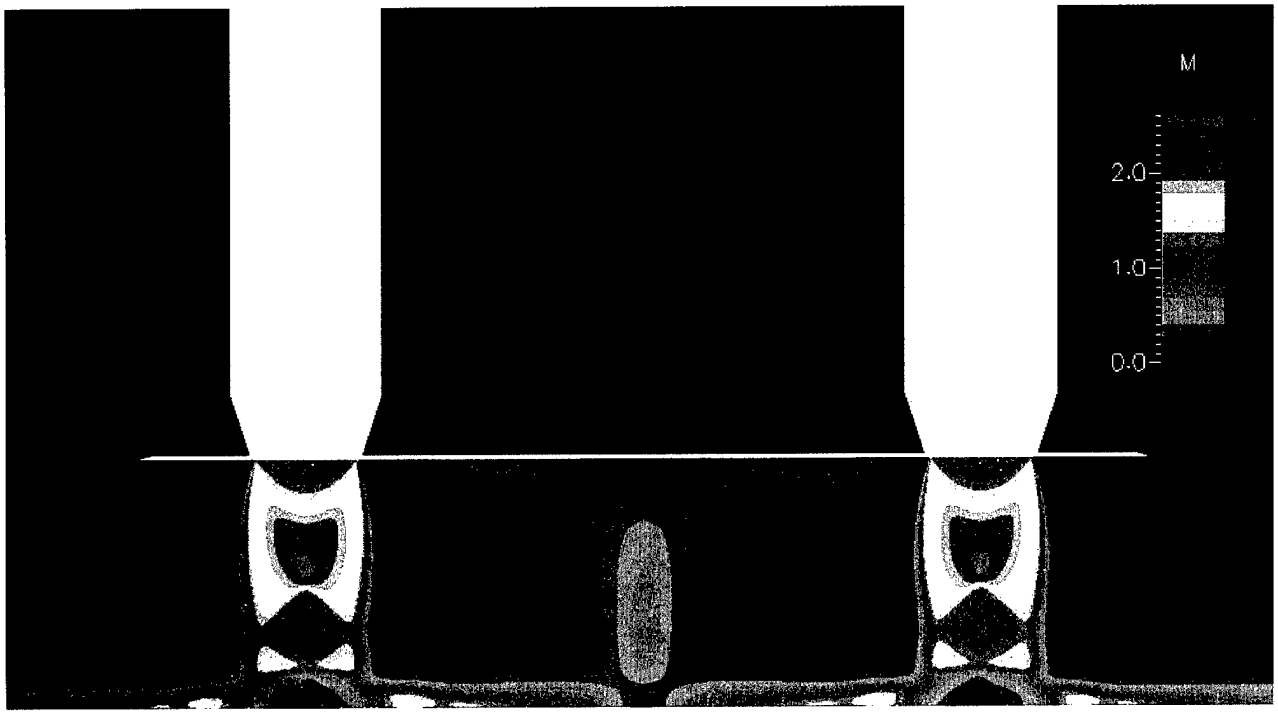


*Figure 3.8. Symmetry Plane Mach Number Contours*

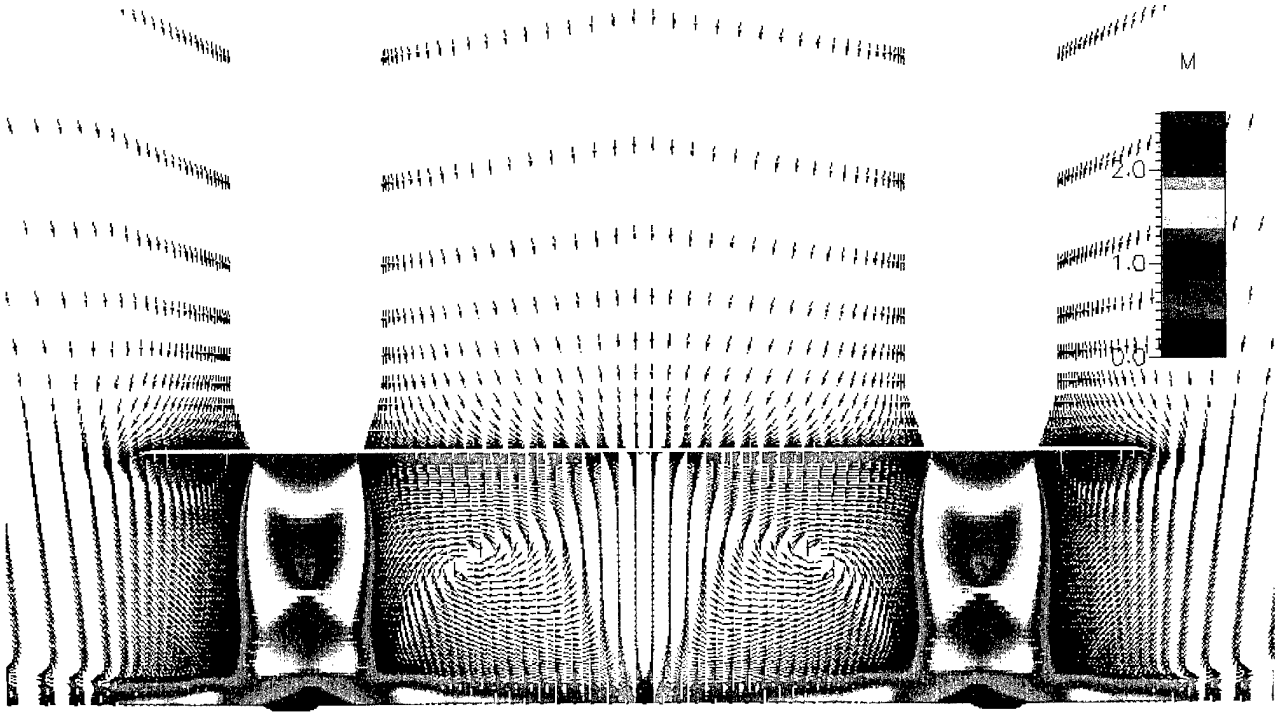


*Figure 3.9. Symmetry Plane Velocity Vectors Colored by Mach Number*

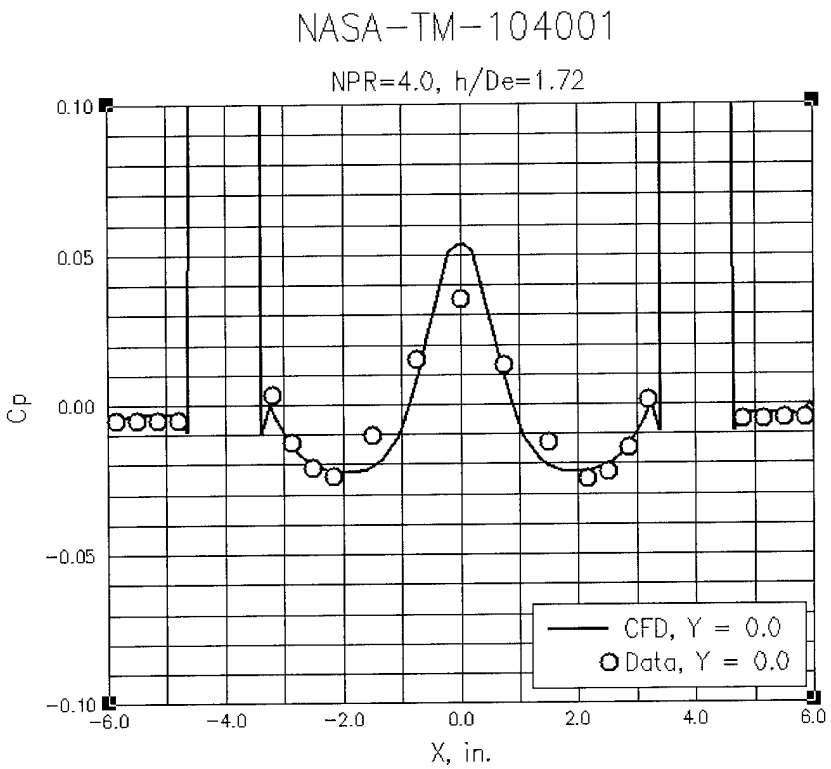


a. Y = 0.0 in.

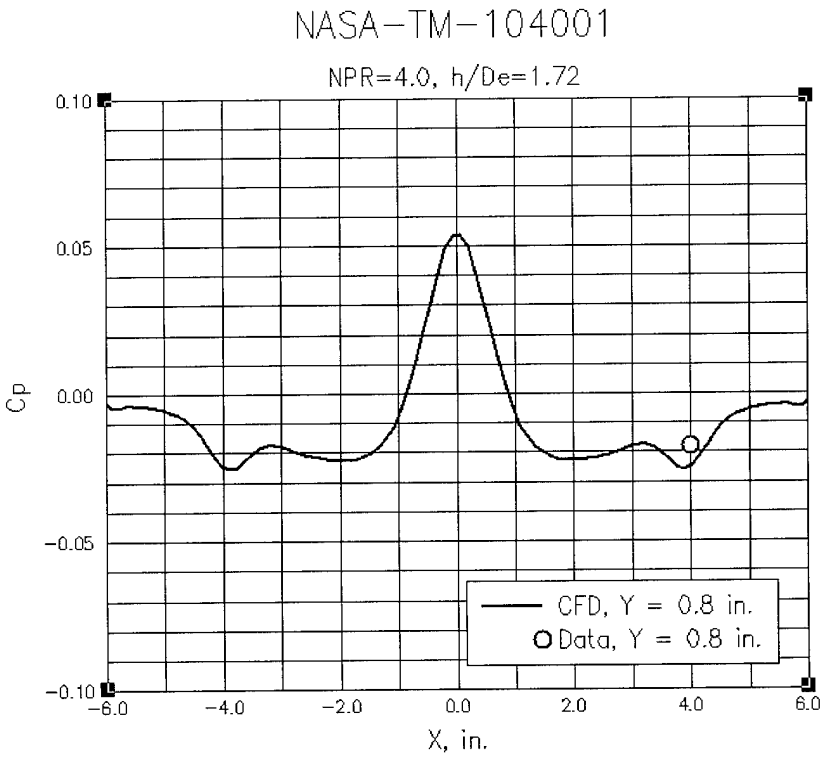


b. Y = 0.8 in.

*Figure 3.10. Comparison of Twin-Jet CFD Predictions to Test Data (cont.)*

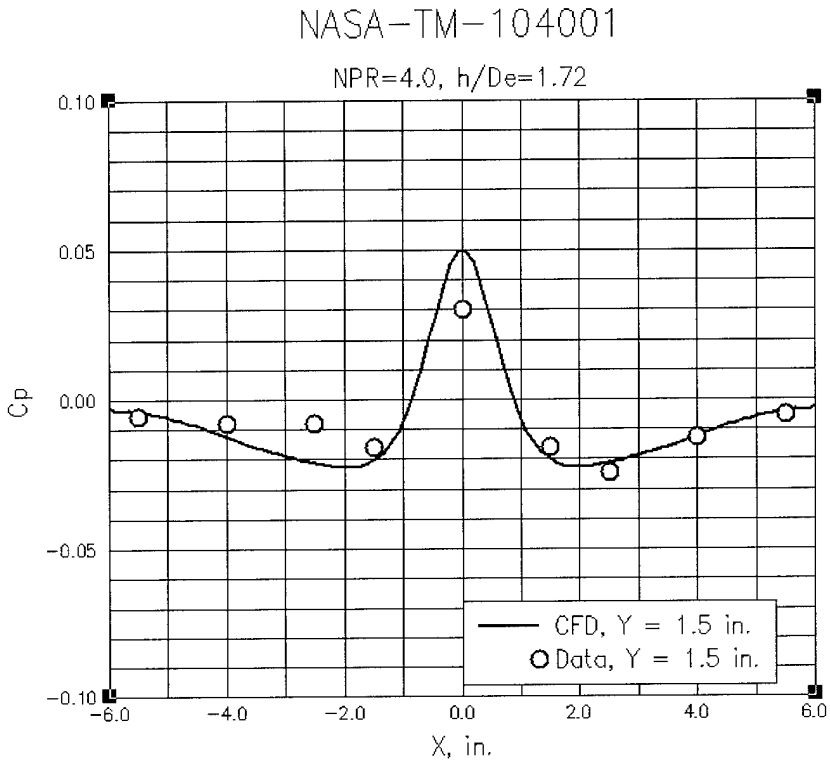


c. Y = 1.5 in.

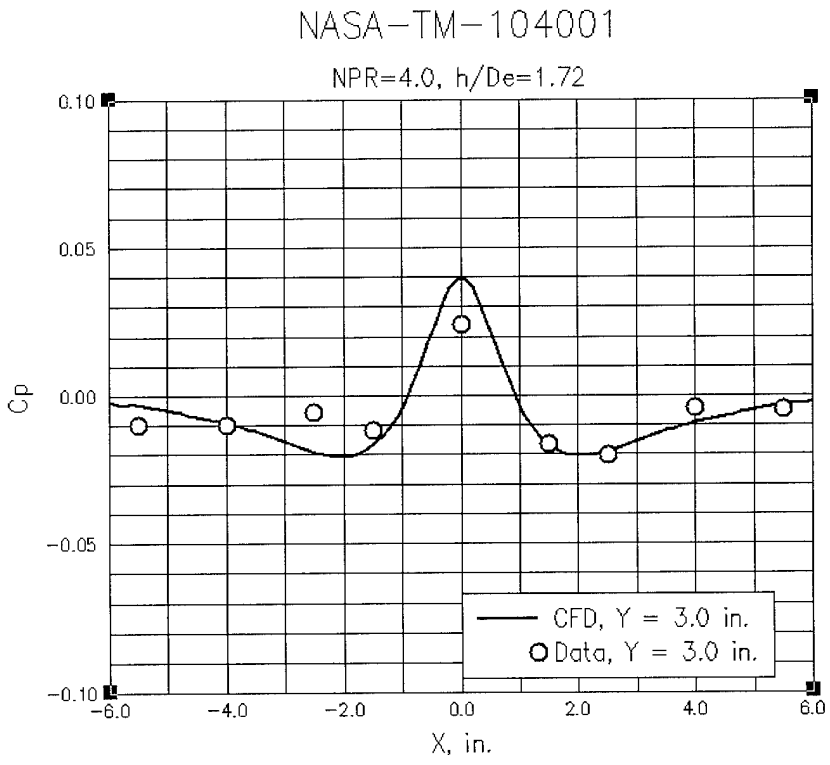


d. Y = 3.0 in.

*Figure 3.10. Comparison of Twin-Jet CFD Predictions to Test Data (concluded)*

## 3.4 Demonstration of X-35B in VSTOL Mode

After the validation of the VSTOL capabilities of the code was finished, a demonstration of the geometric and flow field complexity that could be modeled was desired. Therefore, it was decided that a solution be obtained on an X-35B in hover, as shown in Figure 3.11. To this end, a CAD file containing the geometry for the X-35B aircraft was obtained from the NAWC-AD. However, some difficulties were encountered with the geometry in the file. The file contained no CAD surfaces, only points and lines, as shown in Figure 3.12. When constructing a computational mesh, most grid generation software requires some sort of surface with which the surface points in the mesh are to be associated, but there were no such surfaces in this geometry file. Additionally, the geometry did not incorporate any of the aircraft control surface or nozzle deflections that the X-35B will implement during VSTOL operation, as seen in Figure 3.11. Therefore, to create the mesh, the CFD-GEOM code was used to construct the required surfaces using the points and lines in the CAD file. The deflected control surfaces, nozzles and doors were constructed to more accurately model the X-35B in VSTOL operation, and are shown in Figure 3.13. The surfaces were constructed at CFDRC by the investigating engineer. While these surfaces are only an approximation of the actual aircraft surfaces, it is believed that the fidelity obtained will be adequate for this demonstration. The resulting mesh system was composed of 91 overset and blocked meshes with a total of approximately 1.8 million points. The X-35B surface meshes and outlines of the individual blocks are shown in Figure 3.14.

A viscous solution using the k-ε turbulence model was obtained for the X-35B hovering 3 m. above the ground in stagnant air. The primary inlet, auxiliary inlet, lift fan intake, main exhaust, roll jet exhaust, and lift fan exhaust are flowing, but since no X-35B data was available, the flow rates are approximations. There is no available data for this simulation, but the results are consistent with engineering judgment and demonstrate the ability of CFD-FASTRAN's overset mesh technology to model extremely complex geometries and flow phenomena. A plot of Mach Number contours at the symmetry plane are included in Figure 3.15. The velocity vectors at the symmetry plane are presented in Figure 3.16 and clearly show the upward fountain flow between the two downward jets and several vortices. Figure 3.17 is a plot of Mach Iso-Surfaces colored by the v component of velocity. In Figure 3.17, the fountain is easily identified, as are the plumes from the lift fan, the roll jet, and the main nozzle. Figure 3.18 is a plot of particle traces from the exhausts. This figure demonstrates the complexity of the mixing flow field, showing large vortices at the rear of the aircraft caused by the interaction of the jets.

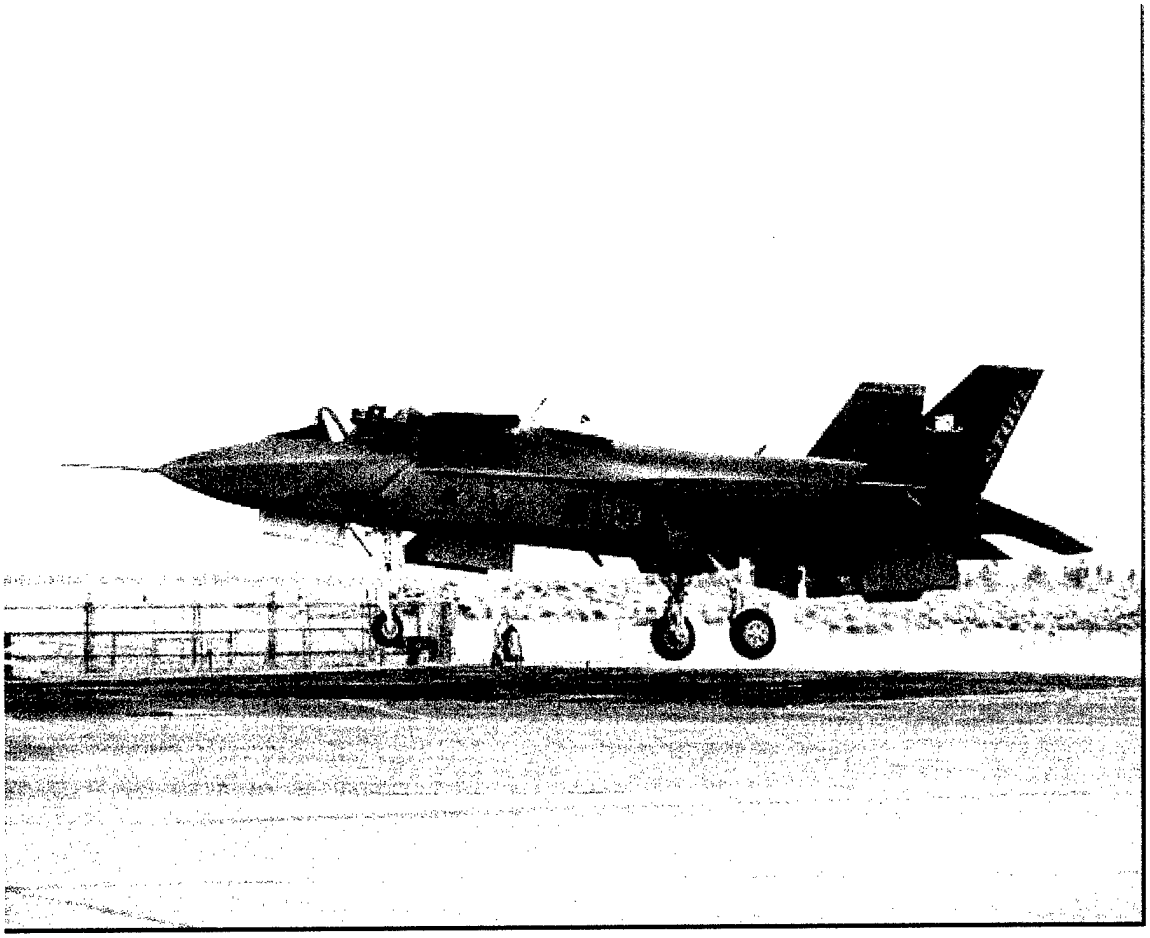

*Figure 3.11. X-35B in Hover, from the Lockheed Martin Aeronautics Company Web Site*

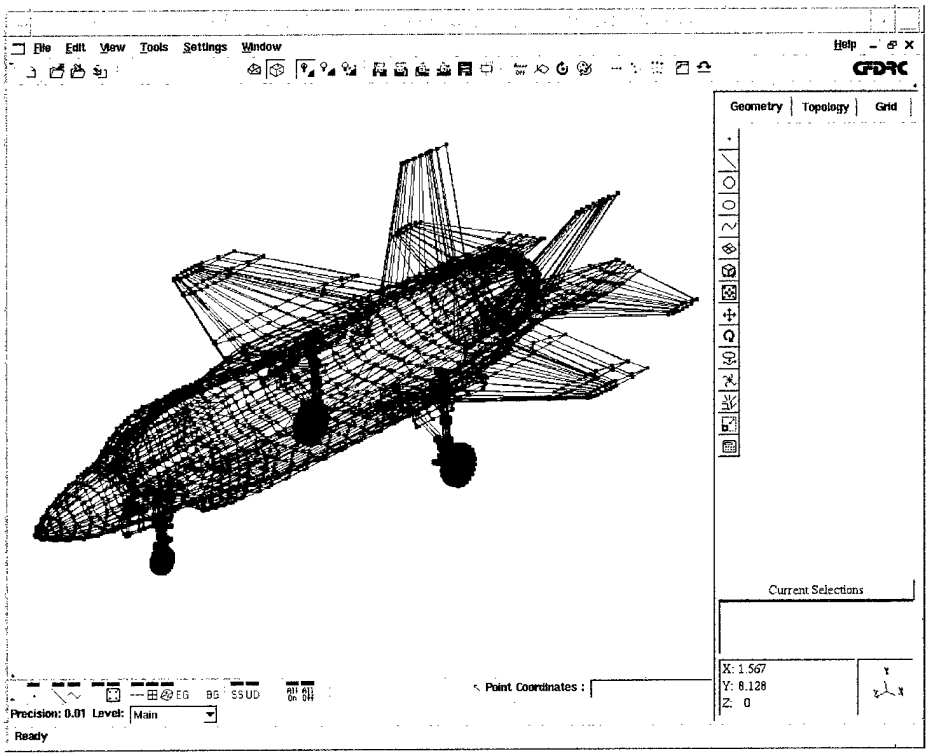


*Figure 3.12. Original X-35B Geometry Received from NAWC-AD*

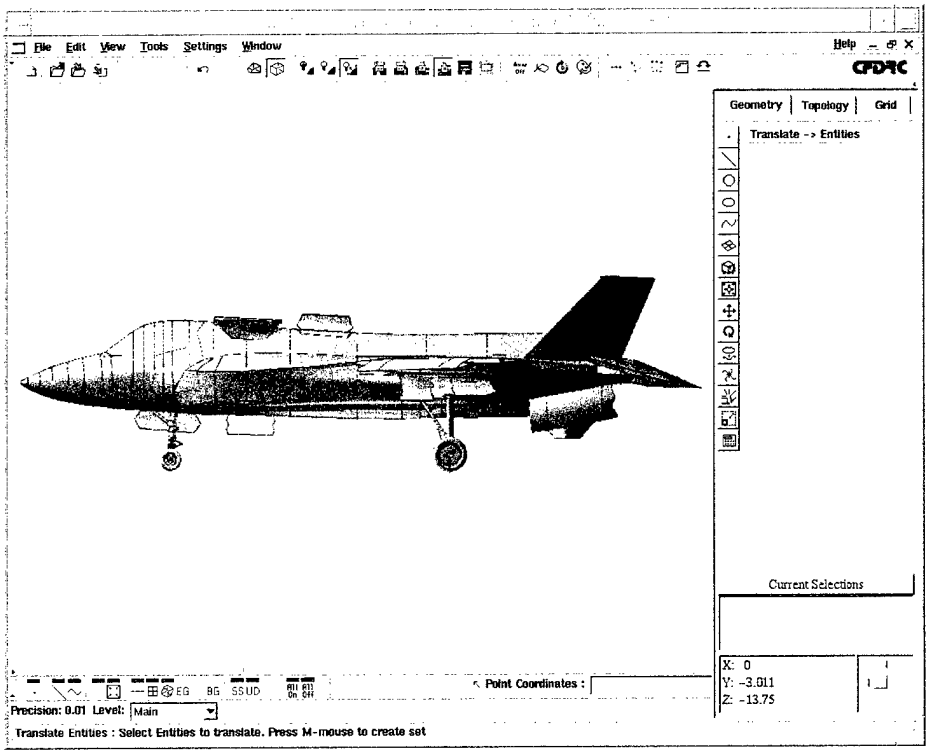


*Figure 3.13. X-35B Surfaces Created at CFDRC*

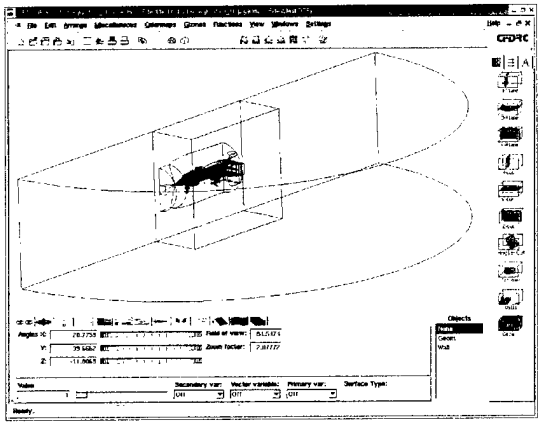

a. X-35B Mesh System

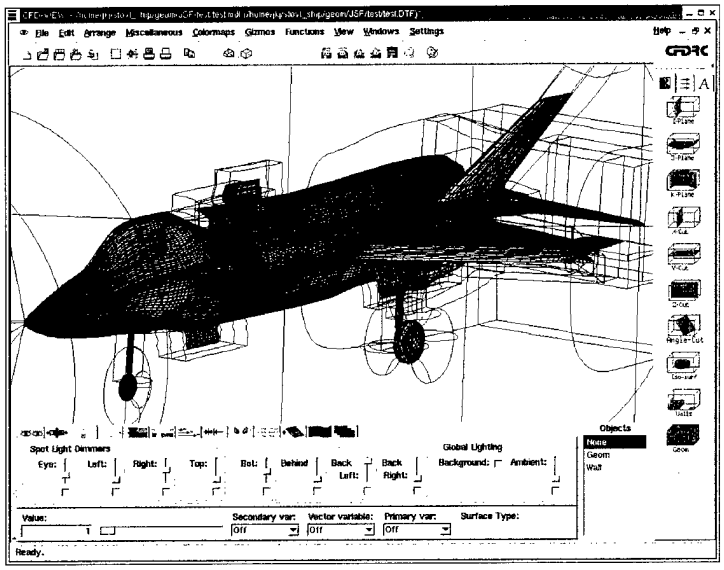

b. X-35B Surface Mesh, Top View

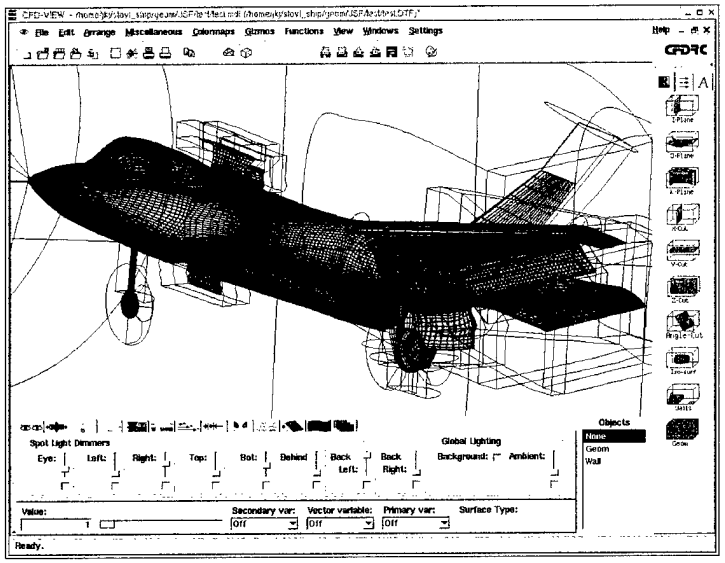

c. X-35B Surface Mesh, Bottom View

*Figure 3.14. Overset Mesh System for the X-35B*

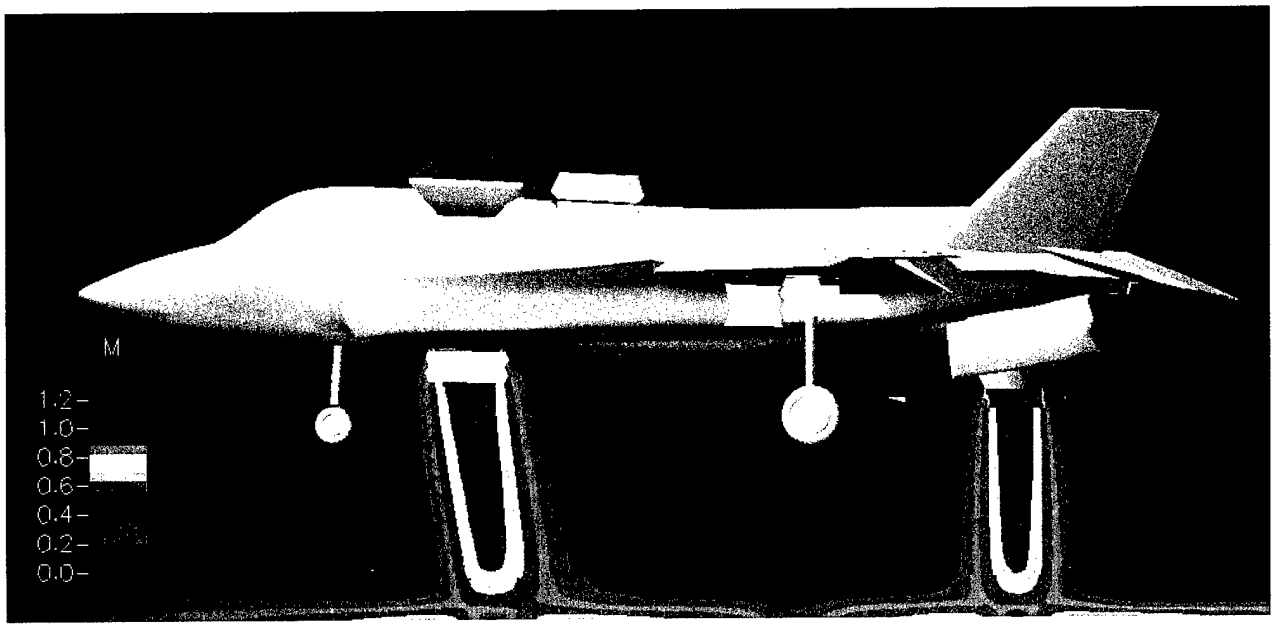


*Figure 3.15. Symmetry Plane Mach Number Contours*

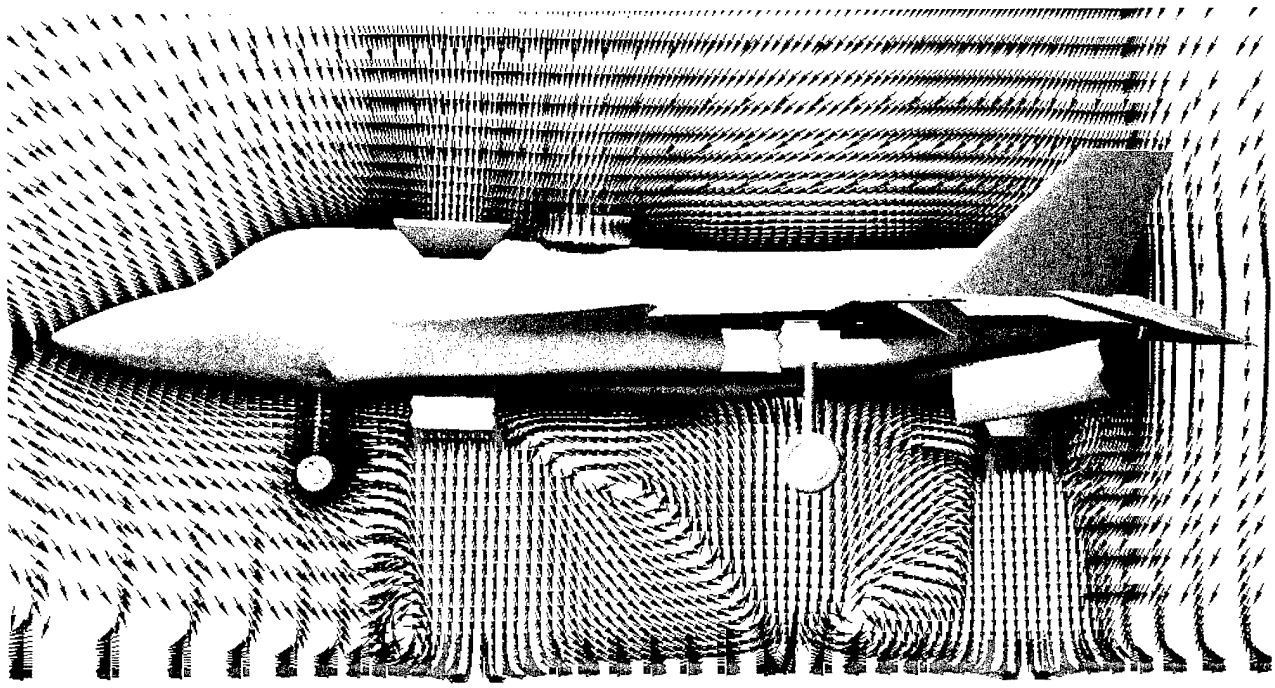

*Figure 3.16. Symmetry Plane Velocity Vectors*

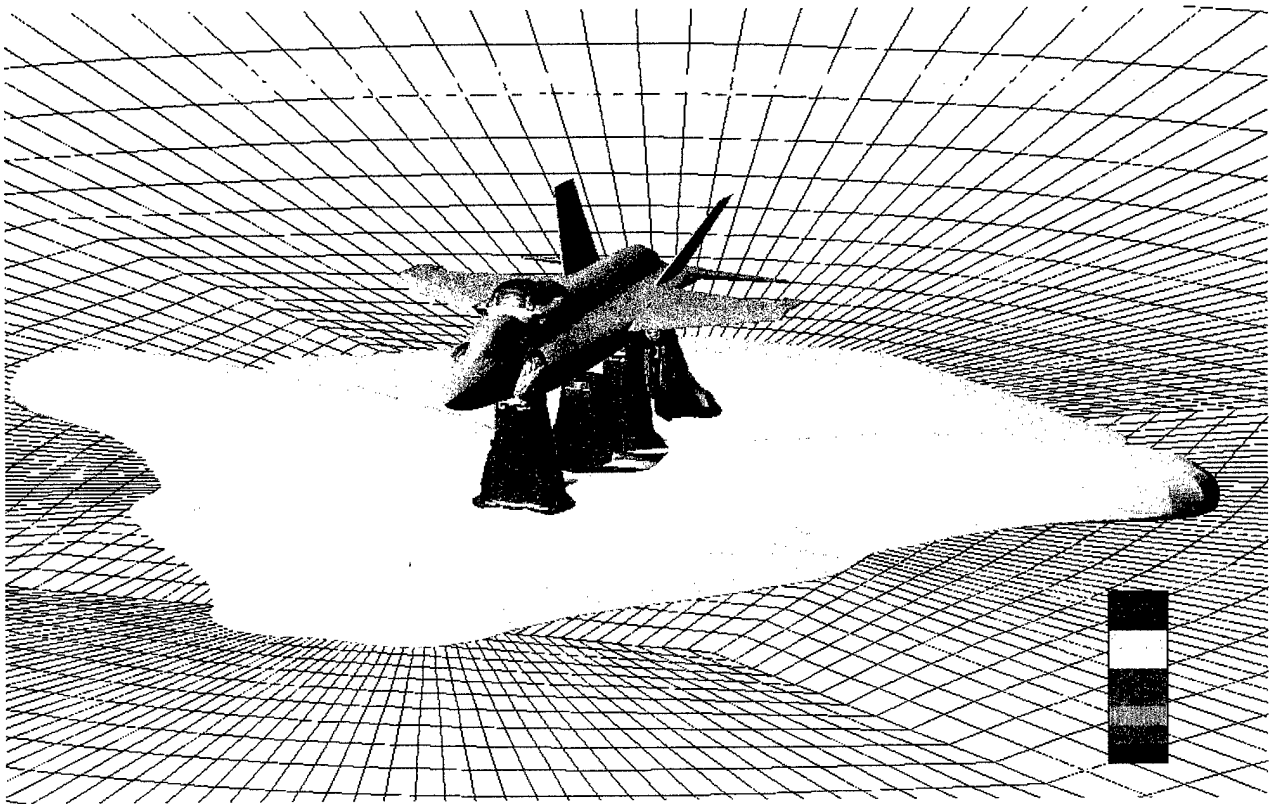

*Figure 3.17. Mach Iso-Surfaces Colored by Velocity*

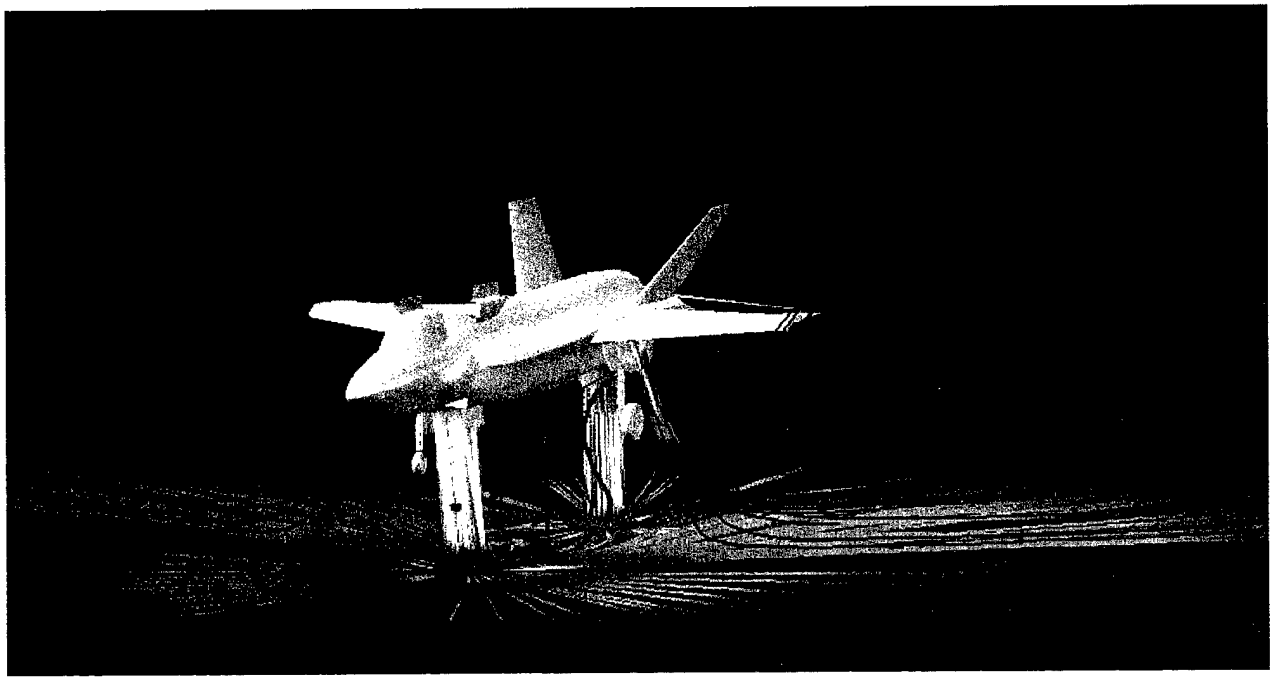

*Figure 3.18. Particle Traces of Lift Fan, Roll Jet, and Main Nozzle Exhausts*

## 4. SHIP AIRWAKE VALIDATION

As discussed in previous sections, a Cartesian mesh approach was selected for the ship airwake validation. This approach was preferred for several reasons. An unstructured Cartesian mesh typically requires less manual labor than a structured mesh. Cartesian meshes have a high volume-meshing efficiency, typically requiring fewer cells than other structured or unstructured mesh approaches for the same spatial resolution and quality of solution. This efficiency in turn translates into lower memory and CPU-time requirements, both of which are major performance criteria for the software environment to be developed in the Phase II work. Lastly, the box-like structures of ships make them especially well suited to a Cartesian approach.

The Cartesian grid generation tool, CFD-VisCART, was used for meshing the ship flow-field. CFD-VisCART is well suited for this type of application particularly because it has several capabilities for generating "viscous layers" (of prescribed thickness and resolution) near surfaces. The box source function was also used extensively to ensure proper mesh density in the regions of interest.

At the beginning of the Phase I work, it was proposed that the CFD-FASTRAN code be used as the solver for the ship airwake flow. However, after some investigations and initial validation studies, it was determined that the pressure-based CFD-ACEU code was more suitable at these low flow velocities. For this reason, coupled with the fact that the CFD-ACEU code would require no Mach scaling for this type of flow, it was decided to use the CFD-ACEU code for all subsequent ship airwake calculations.

The validation studies were performed for two different flow configurations (each involving a different geometry): separated flow over a rib in a channel, and flow over a wind-tunnel model of a ship. The CFD-VisCART grid generation tool was used to generate three different types of meshes for these validation studies. The types of meshes generated were: (i) a stair-stepped Cartesian mesh; (ii) a body-fitted Cartesian mesh; and, (iii) a body-fitted Cartesian mesh with viscous layers.

The stair-step mesh was used with the rib-in-a-channel. A stair-step mesh is constructed exclusively from rectangular cells by successively splitting cells that intersect a surface. Any cell that fully or partially falls inside the geometry is discarded. No effort is made to match the geometry of sloped surfaces. This method was used for the rib-in-a-channel case because a refined stair-step mesh can match the rectangular geometry very well. This type of mesh will typically only approximate the geometry, but is easy to generate and high-quality, orthogonal cells are guaranteed.

A body-fitted mesh with no viscous layers was used with the ship model. In this type of mesh, a stair-step mesh is generated first, and then the nodes of the Cartesian faces nearest the geometry are projected onto the geometry. The new nodes are then used to create faces on the geometry surface, and new cells are constructed between the stair-step cells and the faces lying on the surface. This procedure results in a higher geometric fidelity than that of the stair-step mesh, but results in more skewed cells near and on the surface. The projection of the nodes and the reconstruction of the corresponding cells also introduces the potential for mesh cells with

negative volumes. CFD-VisCART has several integrated tools that can be used to correct these problems if and when they arise.

A body-fitted mesh with viscous layers was also used with the ship model. With this type of mesh, the nodes of the Cartesian faces nearest the geometry are projected onto the geometry, and the reconstructed cell is divided into several thin layers to better define the boundary layer region. Figure 4.1 shows a cut through the three different meshes, illustrating the differences between them.

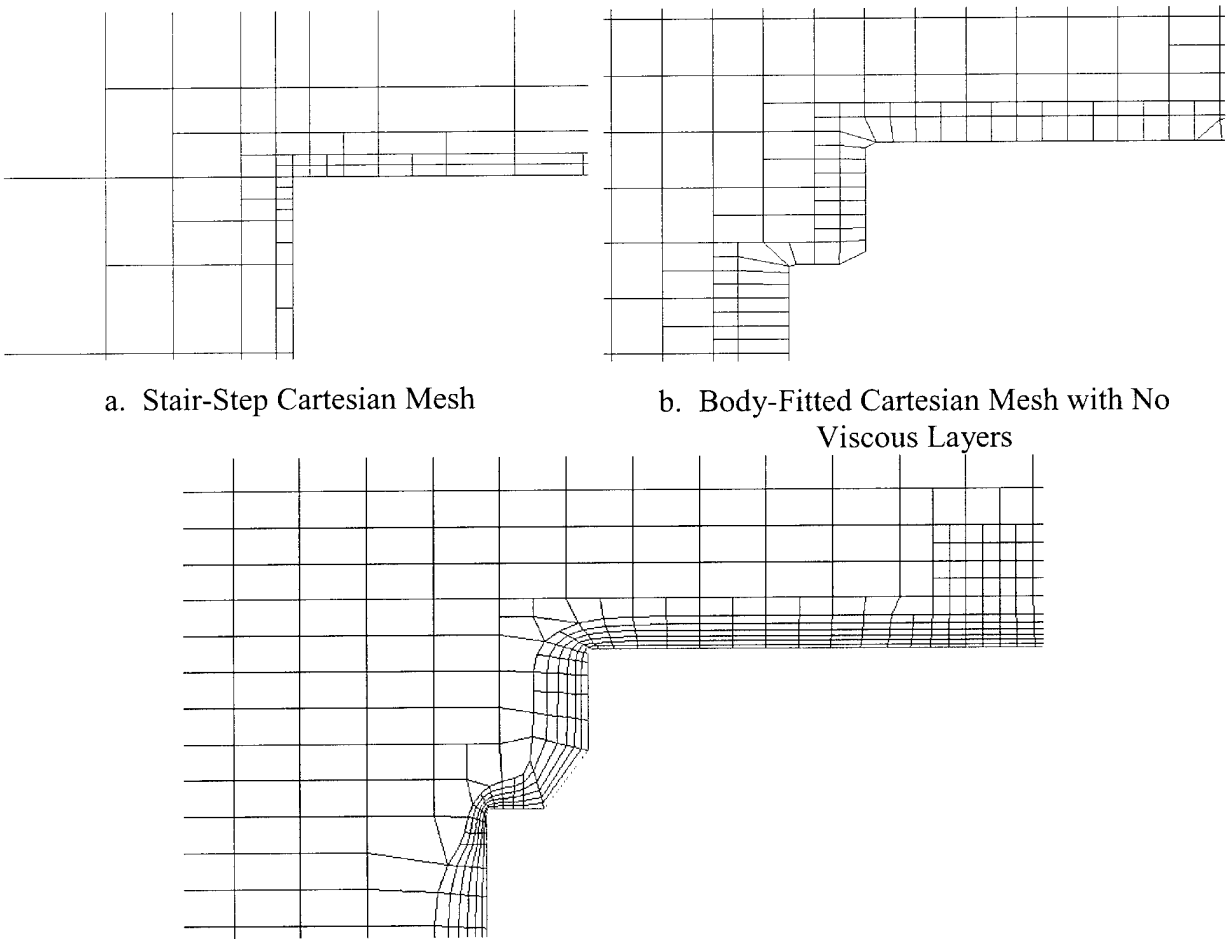

a. Stair-Step Cartesian Mesh

b. Body-Fitted Cartesian Mesh with No Viscous Layers

c. Body-Fitted Cartesian Mesh with Multiple Viscous Layers

*Figure 4.1. Cartesian Mesh Types Utilized for Ship Airwake Validation Calculations*

## 4.1 Rib in a Channel Validations

To begin the validation work, computational predictions were obtained using the CFD-ACEU pressure-based flow solver on a rib-in-a-channel configuration and results were compared to velocity profiles from Reference 18. Reference 18 documents a computational and experimental study of flow over a square rib-in-a-channel. The rib is attached to the bottom of the channel, perpendicular to the flow direction, and spans the entire width of the channel. The test geometry

is shown in Figure 4.2. This test case was chosen because of the similarity of its main features with those of the ship airwake; namely the separation at the front of the body, vortex shedding, large separation regions, and reattachment. The CFD-ACEU flow solver has been validated on similar geometries including flow over a backward facing step. One of these validation results was presented in Section 2 of this report.

This portion of the validation study was composed of several steps. Solutions were obtained using both laminar and LES models and utilizing both structured and Cartesian grid approaches. Both computational grids were run using the same unstructured CFD-ACEU flow solver. The structured mesh was composed of three blocks containing 18100 cells per 2D plane, while the unstructured mesh was composed of 13,600 cells per 2D plane. The mesh spacing normal to the rib surfaces was 1.0e-5 m for the structured mesh. The normal spacing for the stair-step mesh was 3.0e-5 m on top of the rib, and 5.0e-5 m at the front and rear of the rib. Cross-sectional cuts through both grids are presented in Figure 4.3.

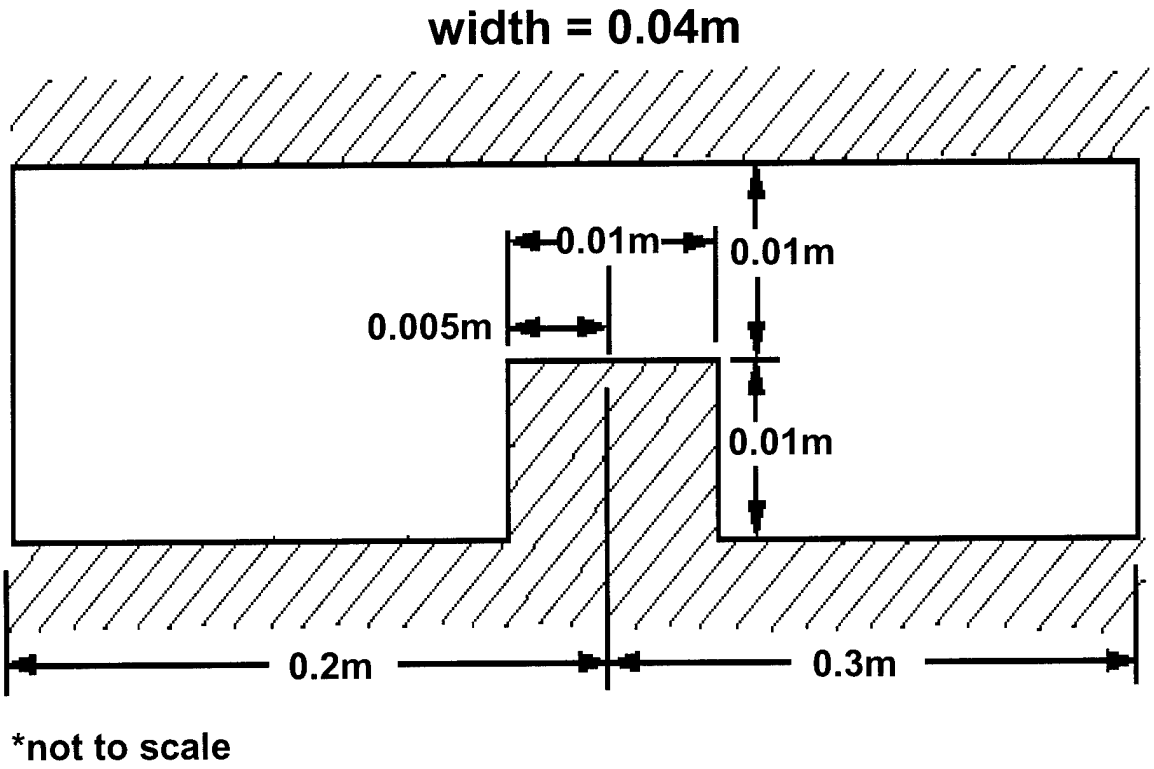


*Figure 4.2. Geometry of the Rib-in-a-Channel*

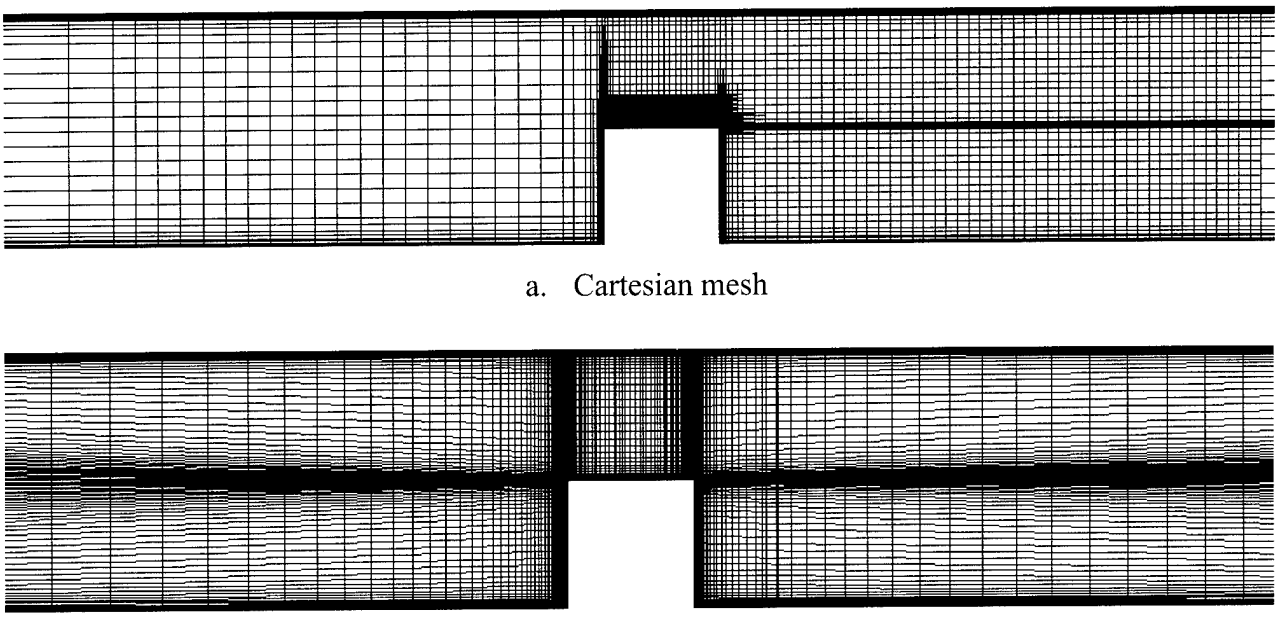

a. Cartesian mesh

b. Structured Mesh

*Figure 4.3. Cross Sections Showing Rib-in-a-Channel Grids*

In Reference 18, the free-stream conditions are reported as a Reynolds number of 42,500 based on the bulk flow velocity and the height of the rib. For this validation study, the conditions chosen to match this Reynolds number were u=62.06 m/sec, P=101325 N/m2, and T=288 K, with the size of the channel and rib shown in Figure 4.2. The test data consisted of averaged velocity profiles at selected stations above the rib and downstream. In this study, the flow was modeled as fully transient, and the resulting velocities at each time step were averaged after the solutions were completed. The procedure for the averaging was to allow the problem to set up for the amount of time required for the bulk flow to pass twice past the last data station, then average the velocities over an equivalent or greater amount of time. The only exception to this procedure was the laminar stair-step Cartesian simulation. This solution was averaged for only half the time of the other cases because of time constraints.

Figure 4.4 shows a comparison of the laminar flow results obtained using the structured and unstructured meshes. In the calculations, the x direction aligns with the flow, the y-axis points from the floor to the ceiling of the tunnel, and the z-axis points from left to right when looking downstream. The origin of the system is at the top mid-point of the rib. The u velocity in Figure 4.4 is non-dimensionalized by the inflow velocity, while the distances are normalized by the rib height, h. In Figure 4.4, both computational predictions match the wind tunnel data reasonably well at the two stations above the rib, with the structured mesh providing slightly superior results. However, neither computational prediction matches the wind tunnel data at x=4.5h, although they match each other closely. It is believed that the laminar prediction is inadequate for predicting the highly turbulent wake and bulk flow separation, and that an LES type model is required.

Figure 4.5 compares the results of the LES solution to those of the previous laminar solution. With the incorporation of the LES model, the simulation agrees well with the wind tunnel data. The agreement at the 4.5h station is especially improved. This demonstrates the ability of the LES model to accurately predict large-scale turbulence separation.

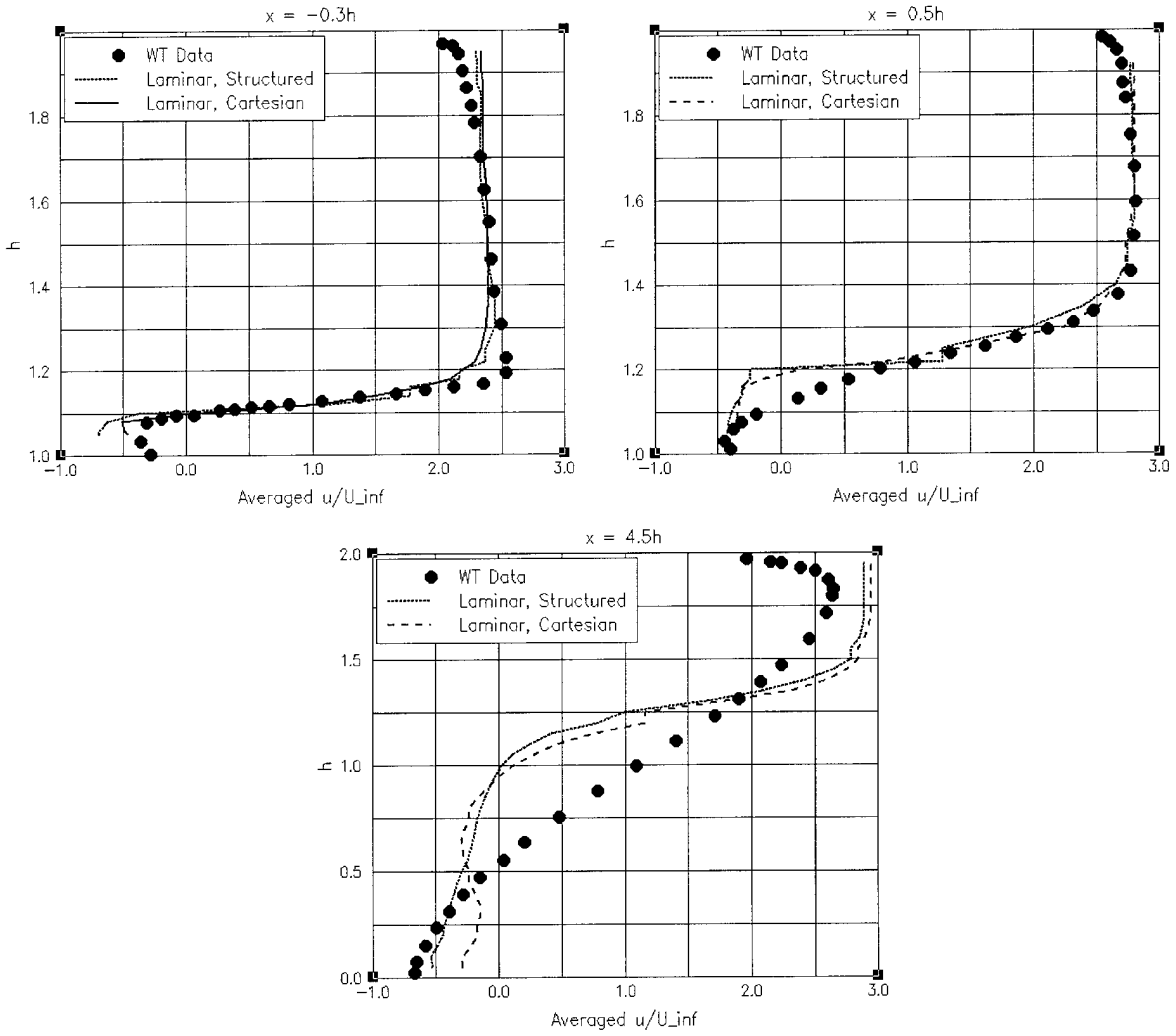


*Figure 4.4. Comparison of Predictions Obtained Using Structured and Unstructured Meshes with Wind Tunnel Data*

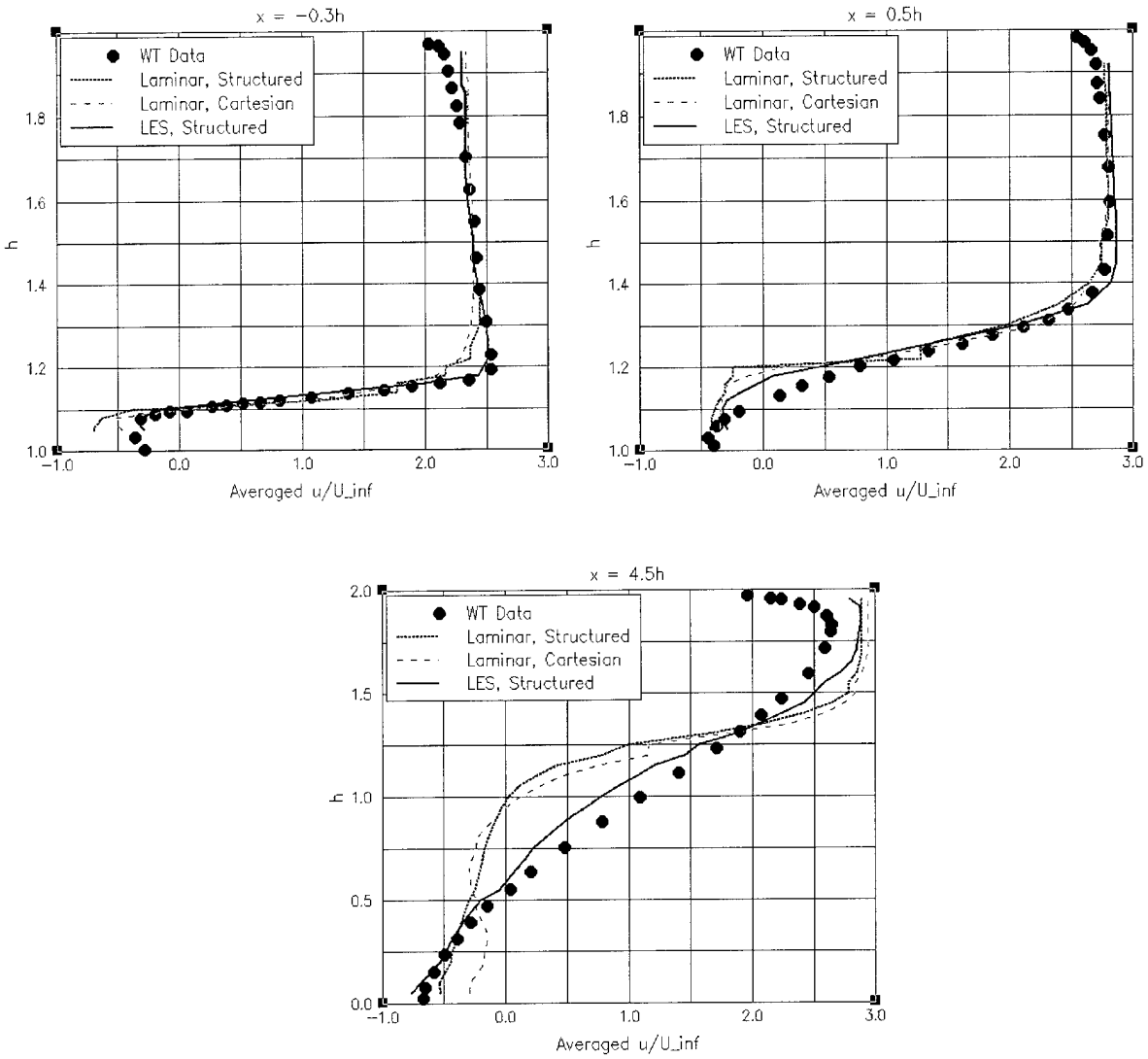


*Figure 4.5. Comparison of Structured Mesh LES Prediction with Wind Tunnel Data*

## 4.2 Tarawa Class LHA

To validate the pressure-based flow solver, CFD-ACEU, for ship airwake prediction with a more geometrically complex case, solutions were also obtained for flow over a 1/120th scale Tarawa Class LHA in a wind tunnel. The LHA surface geometry, the test data, and the free-stream conditions were provided by NAWC-AD. A photograph of an LHA and the corresponding surface geometry are presented in Figure 4.6 and Figure 4.7, respectively. The test was conducted at the NASA Ames Fluid Mechanics Lab wind tunnel, and obtained averaged velocity data in a 2D plane at a constant station 0.5969 m past the bow of the model. The inflow velocity was 51.8 m/sec, at a pressure of 101325 N/m2, and a temperature of 288 K. In the test, the LHA model was 6.8' long, 13.5" tall, and 14.6" wide, and the tunnel test section was 10' long, 32" tall, and 48" wide. To more accurately model the test, the walls of the wind tunnel were included in the simulation so that the model blockage effects would be captured. However, an inviscid wall boundary condition was used on the wind tunnel walls.

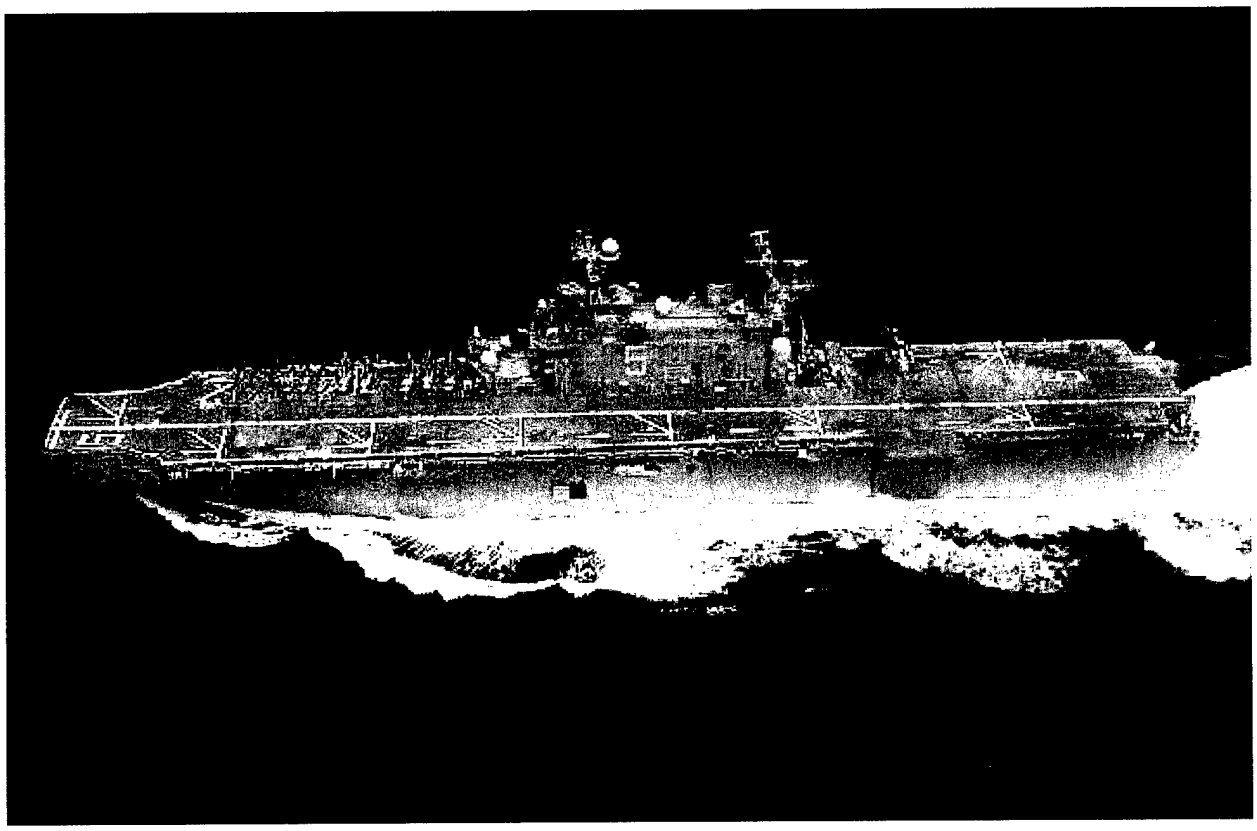

*Figure 4.6. The U.S.S Peleliu, from the U.S.S. Peleliu Website*

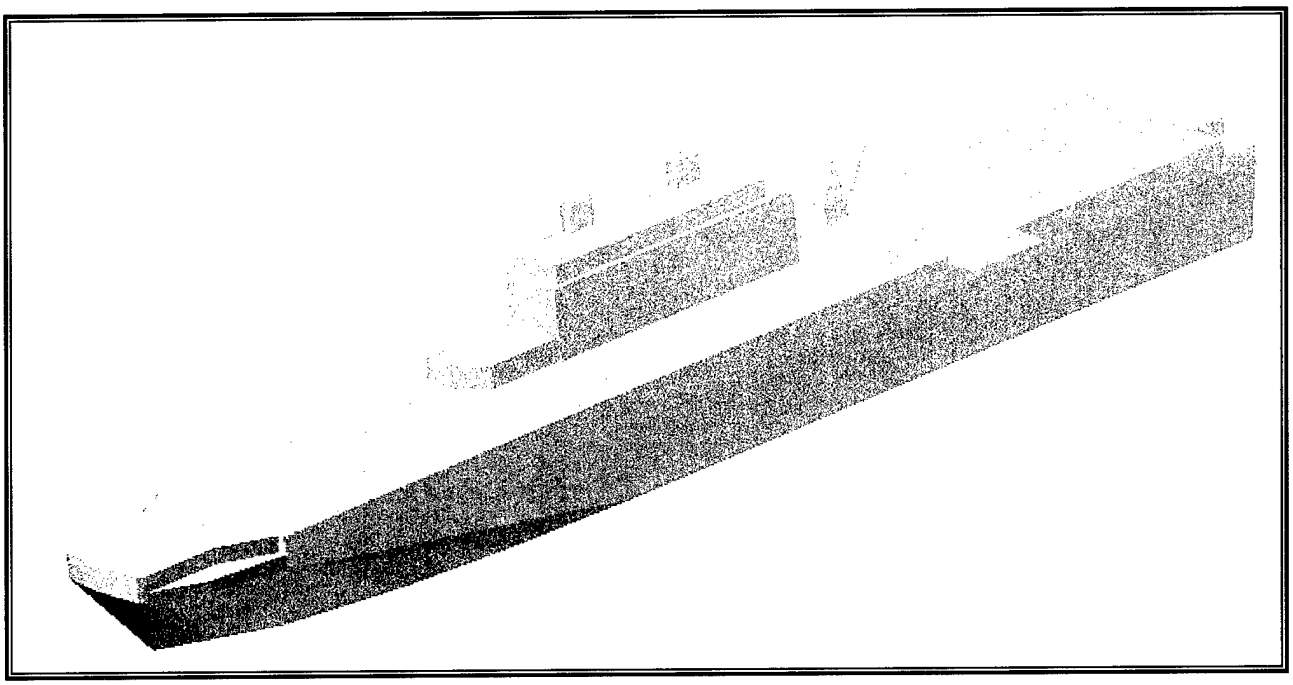

*Figure 4.7. Tarawa Class LHA Simplified Surface CAD Geometry*

Laminar solutions were obtained for this portion of the validation study. In all the LHA solutions, the flow was modeled as transient, and the resulting velocities at each time step were averaged after the solutions were completed. The procedure for the post-processing was to allow the problem to set up for the amount of time required for the bulk flow to pass over the length of the ship twice, then average the values over an equivalent or greater amount of time.

Solutions were obtained with CFD-ACEU using two different types of Cartesian meshes. The first mesh was a body-fitted Cartesian mesh with small spacing off the deck, but no viscous layers. It was thought that this approach would be adequate because the flat deck of the LHA allows the Cartesian mesh to be easily refined to viscous spacing levels. While the spacing off the sides of the hull was not as small, it was thought that the resolution would be adequate to capture the primary vortices. The maximum spacing above the deck for this mesh was 0.001 m normal to the deck, 0.013 m in the streamwise direction, and 0.01 m from port to starboard over the entire length. Some modifications were made to the LHA model to facilitate the construction of this mesh. The small rail-like structure on the port side of the model was removed, and the angle between the hull and the tunnel floor at the bow waterline was increased, as shown in Figure 4.8. Neither change was expected to significantly impact the prediction at the data location. The resulting mesh contained 907,450 points. Cut planes through the mesh are shown in Figure 4.9.

The second mesh was a Cartesian mesh with six viscous layers. The addition of the viscous layers ensures an appropriate viscous spacing off all the body surfaces. More extensive modifications were made to the geometry for the construction of this mesh as well. To ensure good grid quality throughout the computational domain, the crane and aircraft elevator were removed. However, as before, none of the modifications were expected to significantly alter the solution at the data location. Viscous Cartesian grids were generated with the crane and elevator,

but the quality of the cells in those regions was poor. Using box sources and refining the grid in those regions can improve this quality. However to save computational cost, it was decided to remove those two items from the geometry for this calculation. The resulting mesh contained 1,436,316 points. The maximum spacing above the deck for this mesh was 0.01 m in the streamwise direction, and 0.02 m from port to starboard over the entire length. Because of the addition of the viscous layers, the spacing off the entire body was on the order of 0.001 m. Cut planes through the mesh are presented in Figure 4.10. A close-up of the boundary layer region for both the Cartesian meshes is included in Figure 4.11.

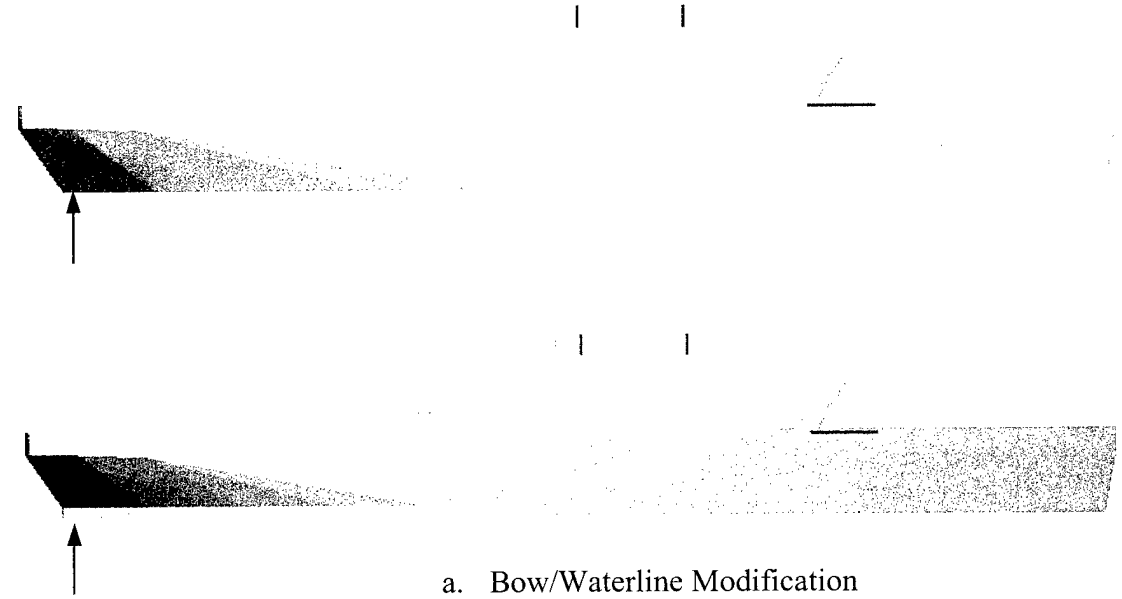

a. Bow/Waterline Modification

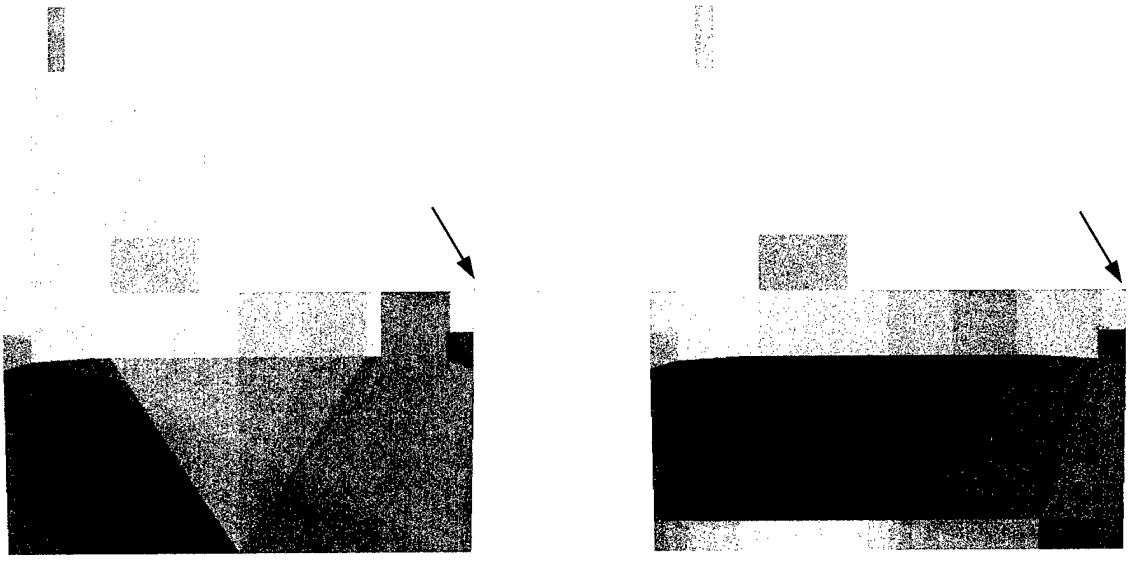

b. Port Side Rail Modification

*Figure 4.8. Geometry Modifications for Body-Fitted Cartesian Mesh*

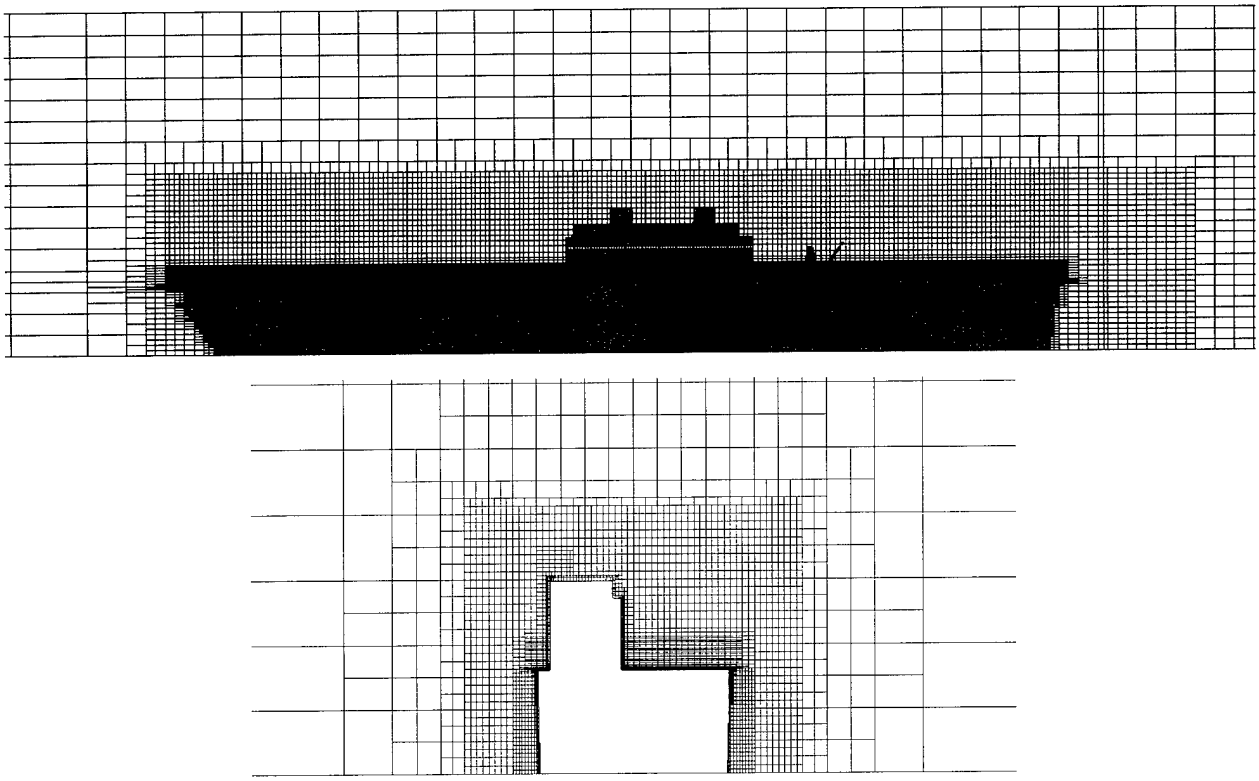

*Figure 4.9. Cut Planes of Cartesian Body-Fitted LHA Mesh with No Viscous Layers*

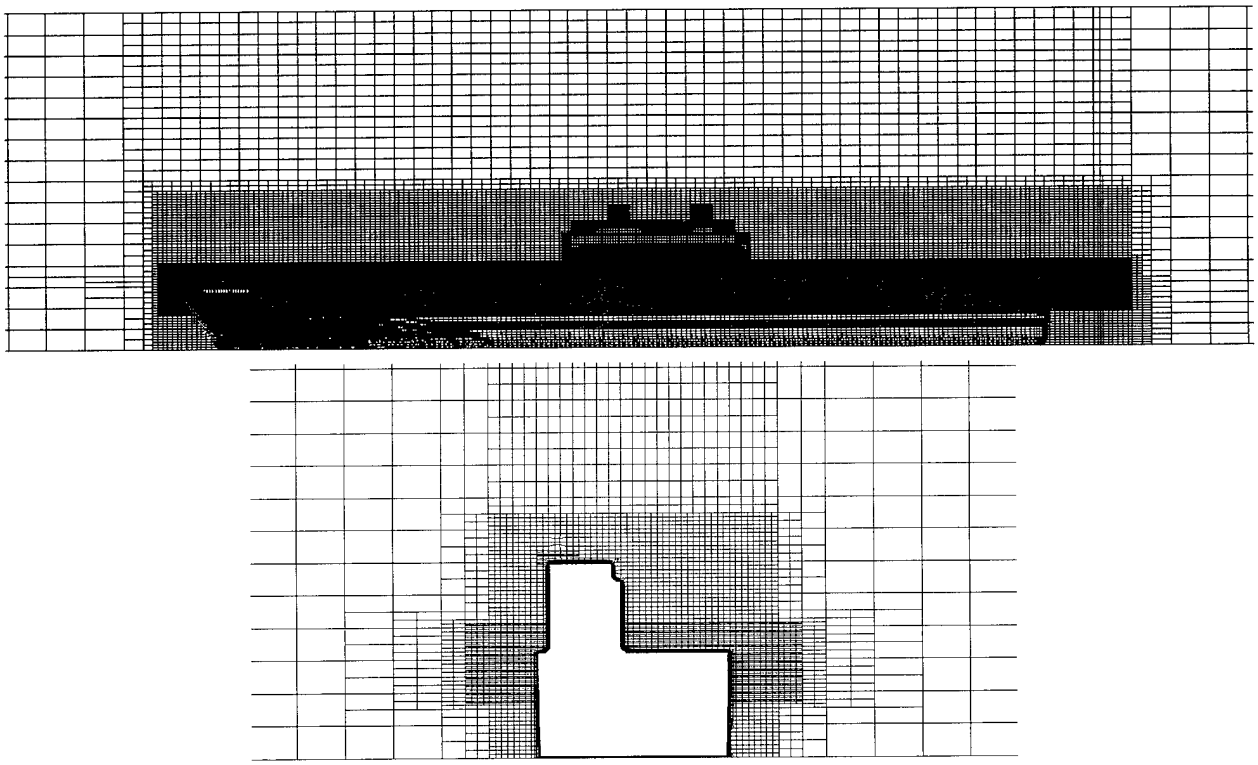

*Figure 4.10. Cut Planes of Cartesian Body-Fitted LHA Mesh with Six Viscous Layers*

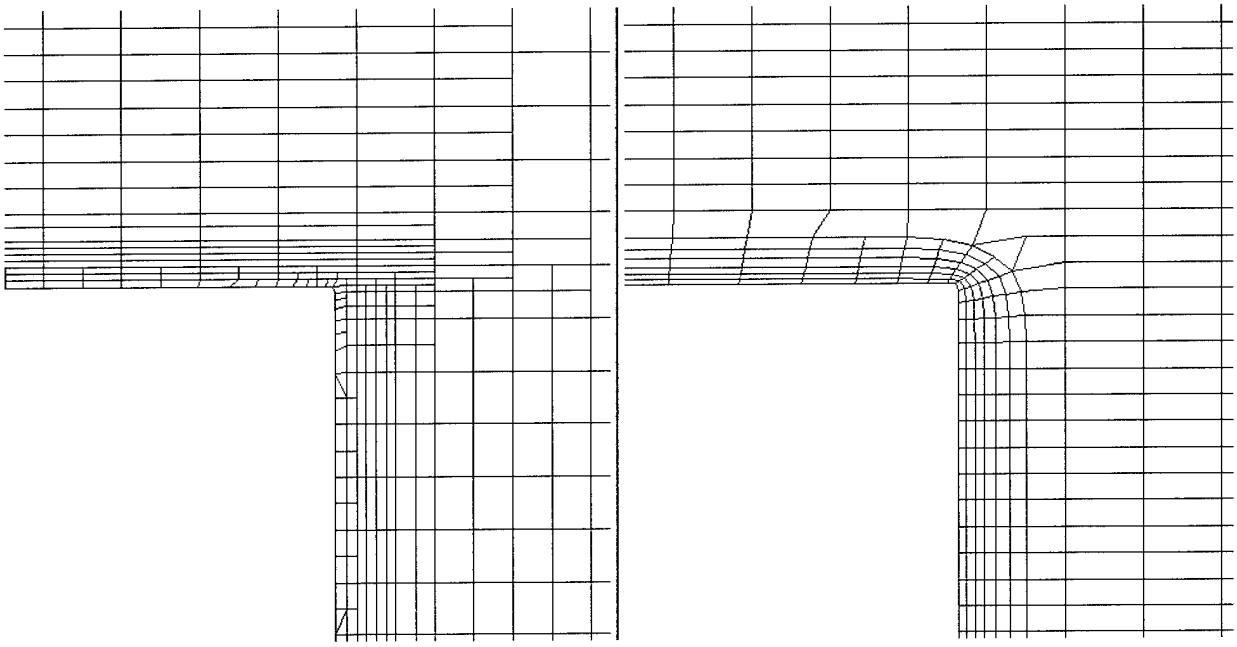

a. Body-Fitted with No Viscous Layers b. Body-Fitted with Six Viscous Layers

*Figure 4.11. Comparison of the Boundary Layer Regions in the Body-Fitted Cartesian Meshes*

Velocity contours at the ship centerline are included in Figure 4.12, and illustrates the large separated regions that are present. Once again, these plots are at an instant in time and are not averaged.

The CFD-ACEU average velocity predictions for both LHA mesh types are compared to the wind tunnel data in Figure 4.13. Both solutions match the velocity distribution reasonably well. The location and velocity of the separated region running down the center of the deck is captured, while the vortices on the port and starboard sides are present, but are slightly outboard with lower u velocity components. As the distance off the deck increases and the flow approaches free stream conditions, the agreement between the test data and computational predictions improve. As can be seen from the figures, the six-layer viscous mesh provides only a slight improvement. This result was unexpected. It was thought that the six-layer mesh would capture the side vortices much better than the zero-layer mesh. However, this might indicate that the viscous layers are not necessary, and that the better quality and more economical zero-layer mesh may be adequate. As was the case for the rib-in-a-channel, it is expected that the addition of the LES model would appreciably enhance the solution.

Mesh densities for the ship airwake validation calculations were determined by engineering judgments and from previous experience. Proper mesh refinement studies were not possible because of time constraints. Mesh refinement studies are proposed for the Phase I Option and for Phase II of this program.

a. Velocity Contours for the Body-Fitted Cartesian Mesh with No Viscous Layers

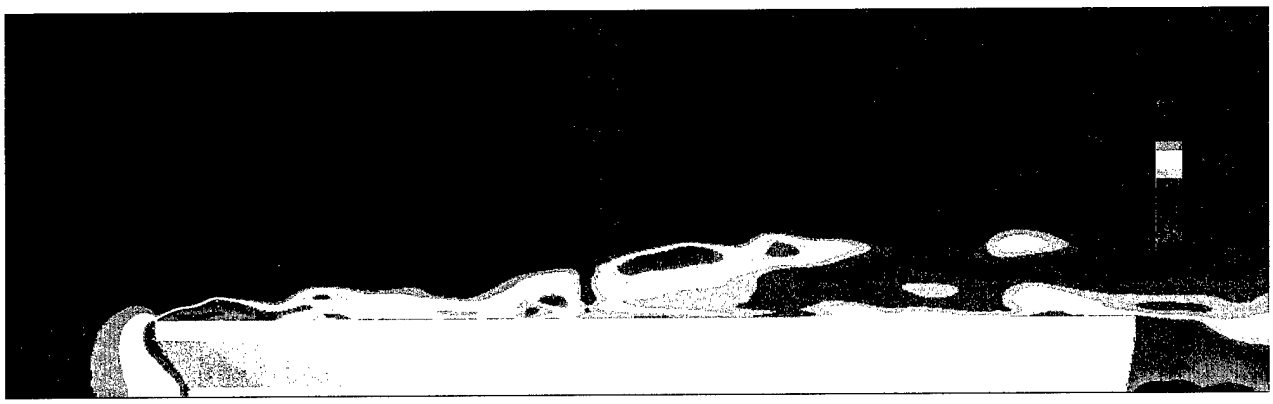

b. Velocity Contours for the Body-Fitted Cartesian Mesh with Six Viscous Layers

*Figure 4.12. Velocity Contours at LHA Centerline*

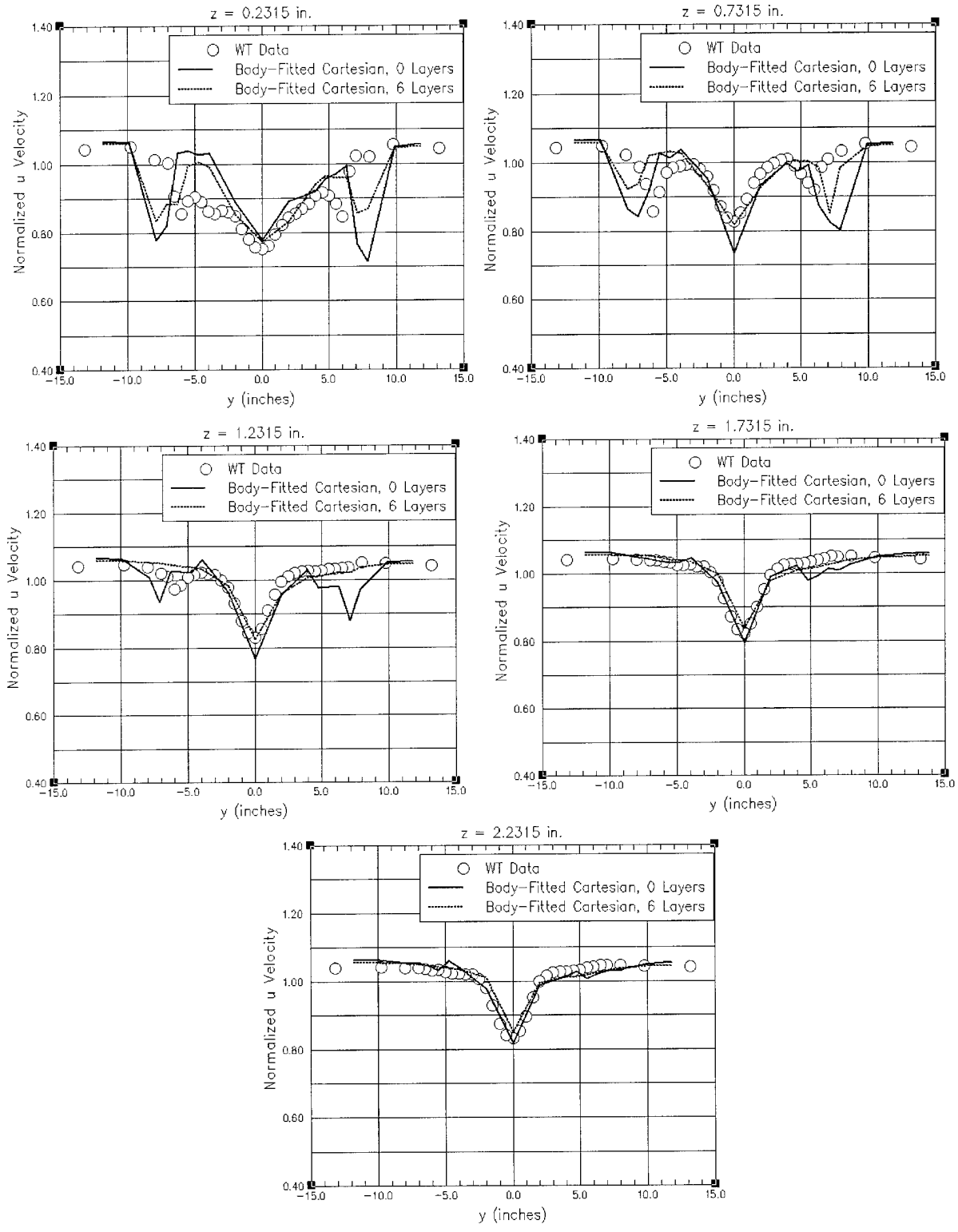


*Figure 4.13. Comparison of Cartesian Mesh LHA u-Velocity Predictions to Wind Tunnel Data*

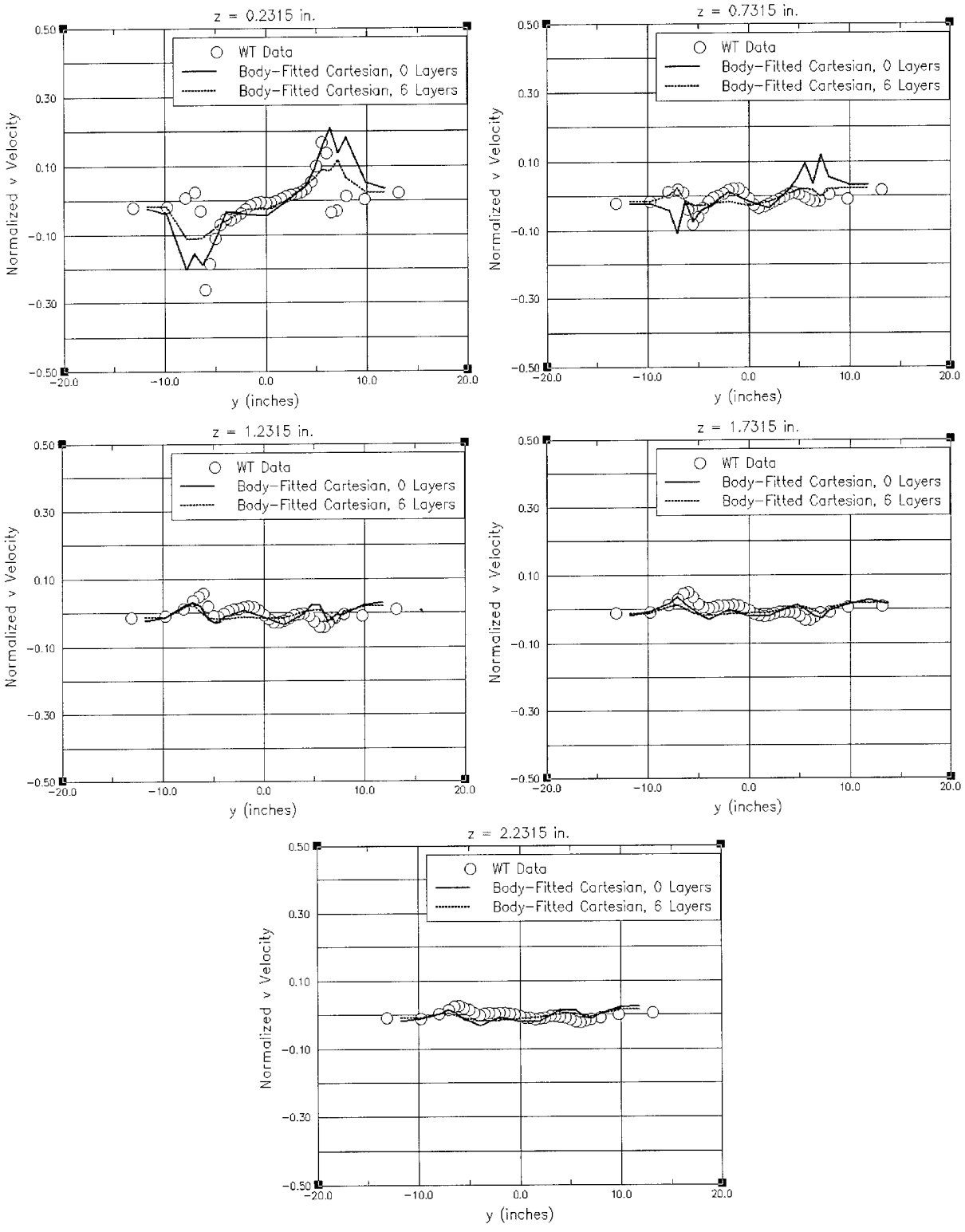


*Figure 4.14. Comparison of Cartesian Mesh LHA v-Velocity Predictions to Wind Tunnel Data*

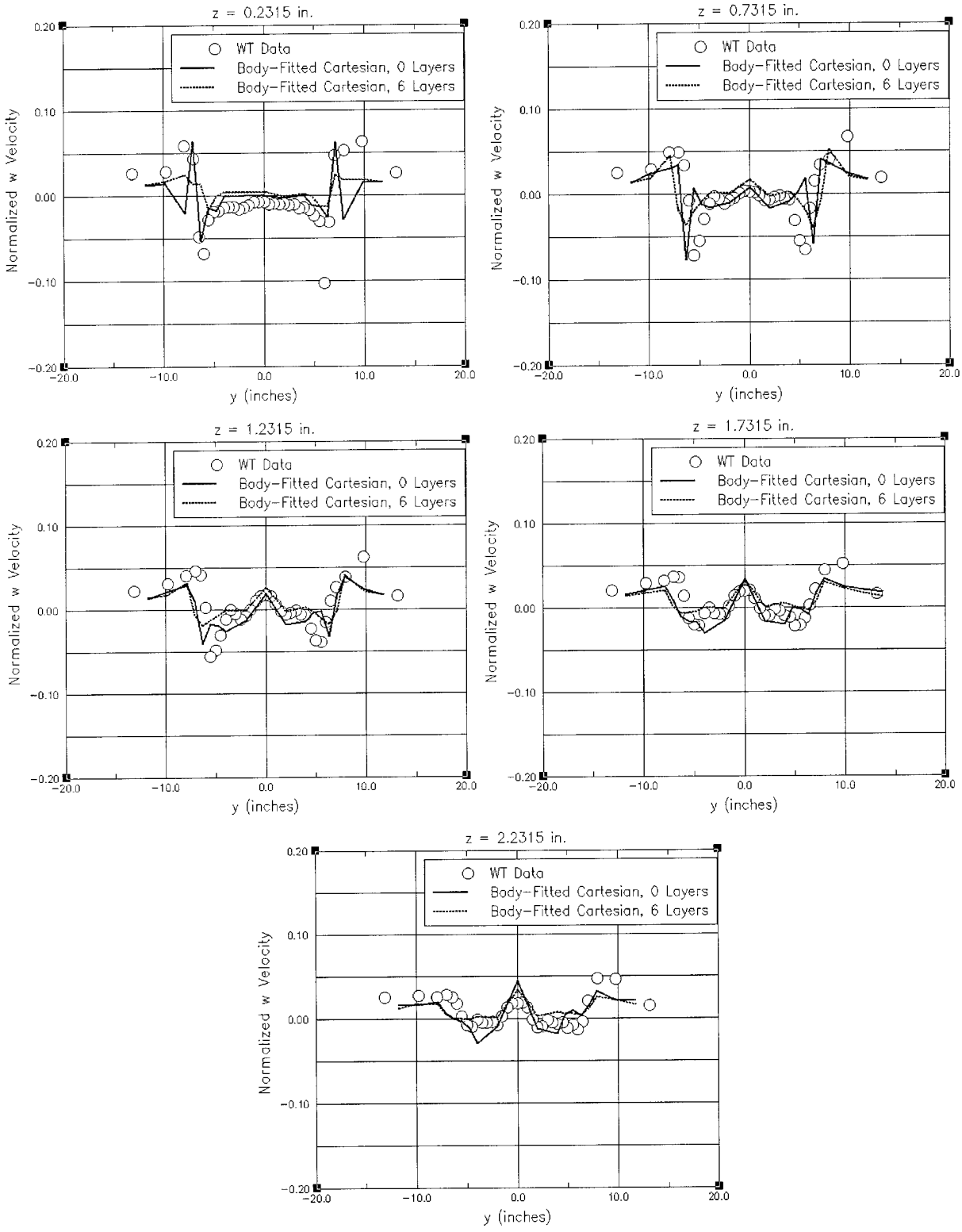


*Figure 4.15. Comparison of Cartesian Mesh LHA w-Velocity Predictions to Wind Tunnel Data*

# 5. COUPLED VSTOL AIRCRAFT/SHIP DEMONSTRATION

As outlined earlier in this report, a major feature of the methodology proposed for the Phase II work is the enabling of different solvers to perform computations on different sub-grids of the overall computational domain. This approach makes it possible to deploy different solvers in the flow regimes in which they are most effective and efficient. This is expected to provide several practical advantages for simulating the multi-regime flows encountered in VSTOL-ship configurations. The specific recommended combination of solvers for coupled VSTOL-ship calculations utilizes the pressure-based solver CFD-ACEU for the lower-speed flow over the ship, and the density-based solver CFD-FASTRAN for the higher-speed flow about the aircraft.

A crucial link in the multi-solver approach described above is the coupling between the different solvers: this must be efficient, accurate, and robust, and must establish a very high degree of actual numerical coupling between the solutions on different grids, with little loss in the overall time-accuracy or the degree of implicitness of the solution across the whole system of component grids. The coupling will be accomplished in this work through the chimera technique, which is one of the most effective and widely-used techniques for coupling solutions on different grids (though usually using the same solver throughout).

Since the ship and VSTOL grids may be of very different types, and may contain arbitrary polyhedral cells, the chimera implementation required in this work must be able to handle any type of cell and grid. This capability is already available within an arbitrary-mesh chimera module developed at CFDRC, and has already been demonstrated for coupling solutions on different unstructured grids, but not using CFD-FASTRAN. In the Phase I work here, the module was extended to enable the coupling of CFD-FASTRAN and CFD-ACEU for the first time.

After completion of the software extensions and preliminary testing, the unstructured-mesh chimera module was tested on a VSTOL-ship configuration, comprising a structured grid for the aircraft overlaid on a Cartesian grid for the ship. The purpose of the test was to establish the correct operation of the module, and to demonstrate that the two very different solvers can be coupled together to give a continuous solution. Figures 5.1 and 5.2 show the holes cut in the aircraft mesh by the ship (missing cells), and the hole in the ship by the aircraft (blue to orange region), respectively. Figure 5.3 displays unit velocity vectors colored by downward velocity at the centerline of the configuration. The coupling between the downward-directed jet of the aircraft and the induced vortices and impingement flow patterns on the ship grid are clearly visible. Figure 5.4 shows a close up of the solution around the interface between the two grids. The extension of the visualization software to unstructured overset meshes is not yet complete, as can be seen from some of the vectors in the Cartesian mesh hole. Nevertheless, the figure shows the continuity of the solution and the velocity vector plots across the interface between the two grids (and hence the solution domains of the two different solvers). The test demonstrates the applicability of the unstructured mesh chimera module to the task assigned to it for the Phase II work, and clearly establishes that a density-based and pressure-based solver can be coupled together in the manner proposed for the Phase II. Despite this initial success, there are still some technical issues that must be resolved for such couplings, and these will be addressed in the Phase II work.

The unstructured chimera module uses several state-of-the-art techniques for acceleration of the geometric and data-transfer operations, making it ideally suited to meet the efficiency and fast turn-around objectives of this work. Additional details regarding the algorithm and implementation details of the unstructured chimera module are given in Reference 8.

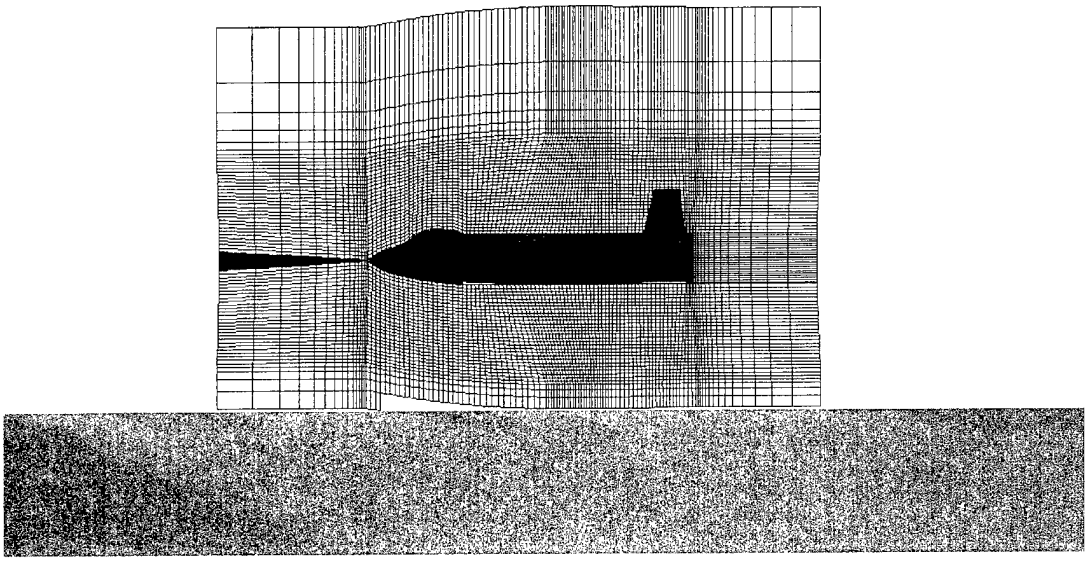

*Figure 5.1. Hole Cut in Aircraft Mesh by the Ship*

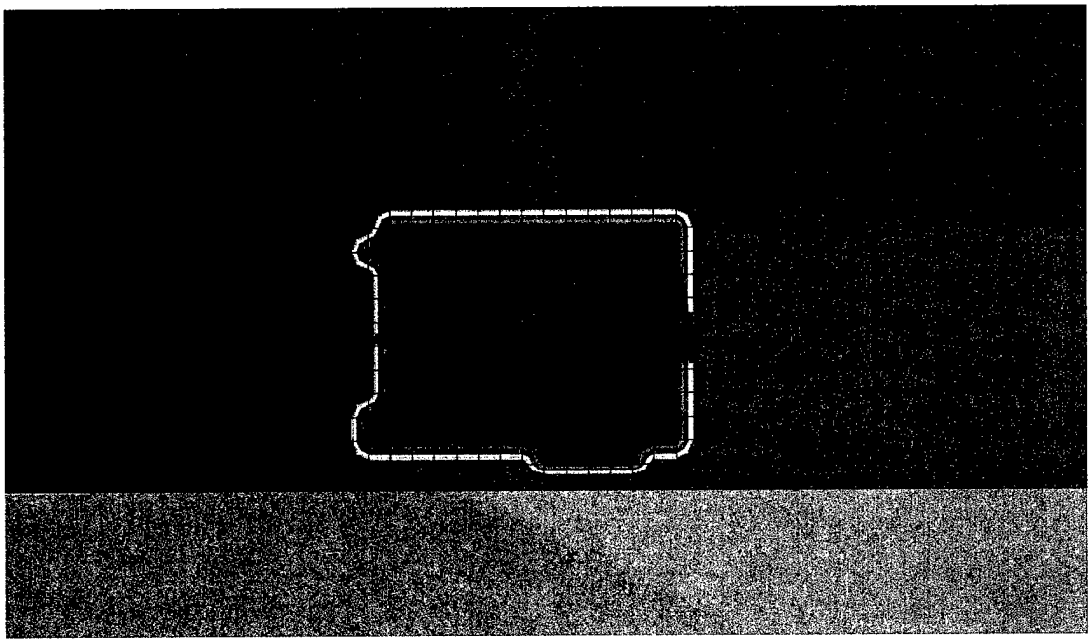

*Figure 5.2. Hole Cut in the Ship Mesh by the Aircraft*

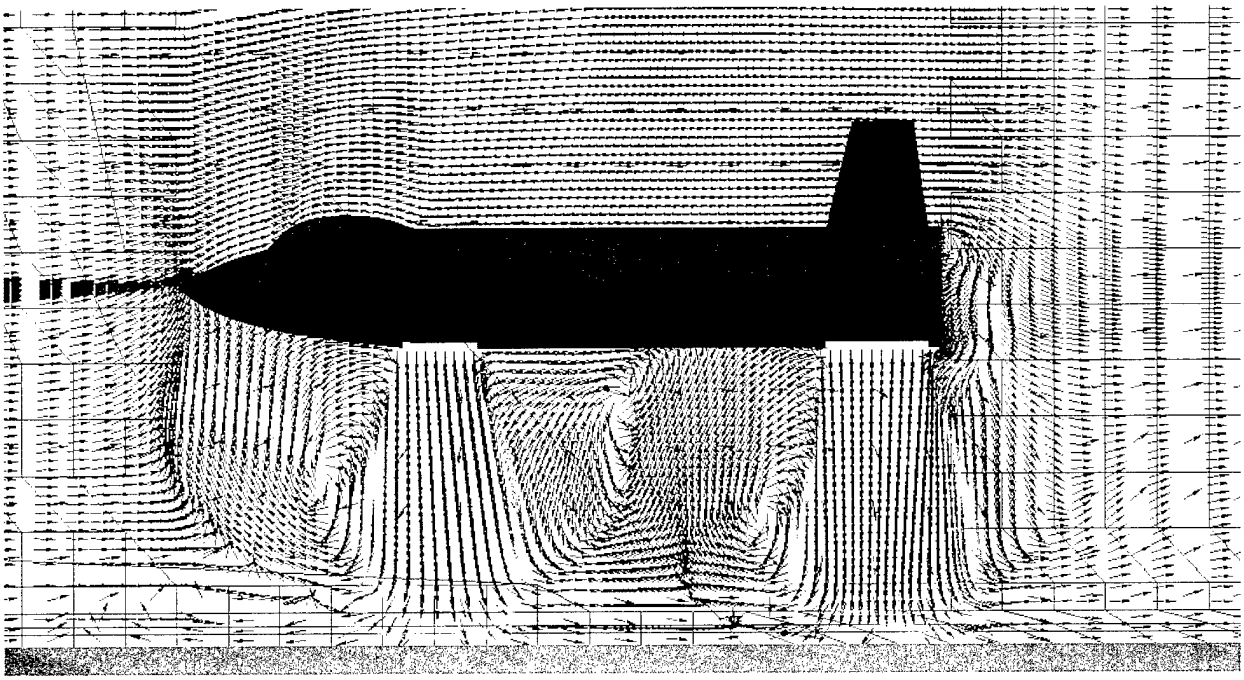

*Figure 5.3. Coupled VSTOL Aircraft/Ship Unit Velocity Vectors Colored by Downward Velocity*

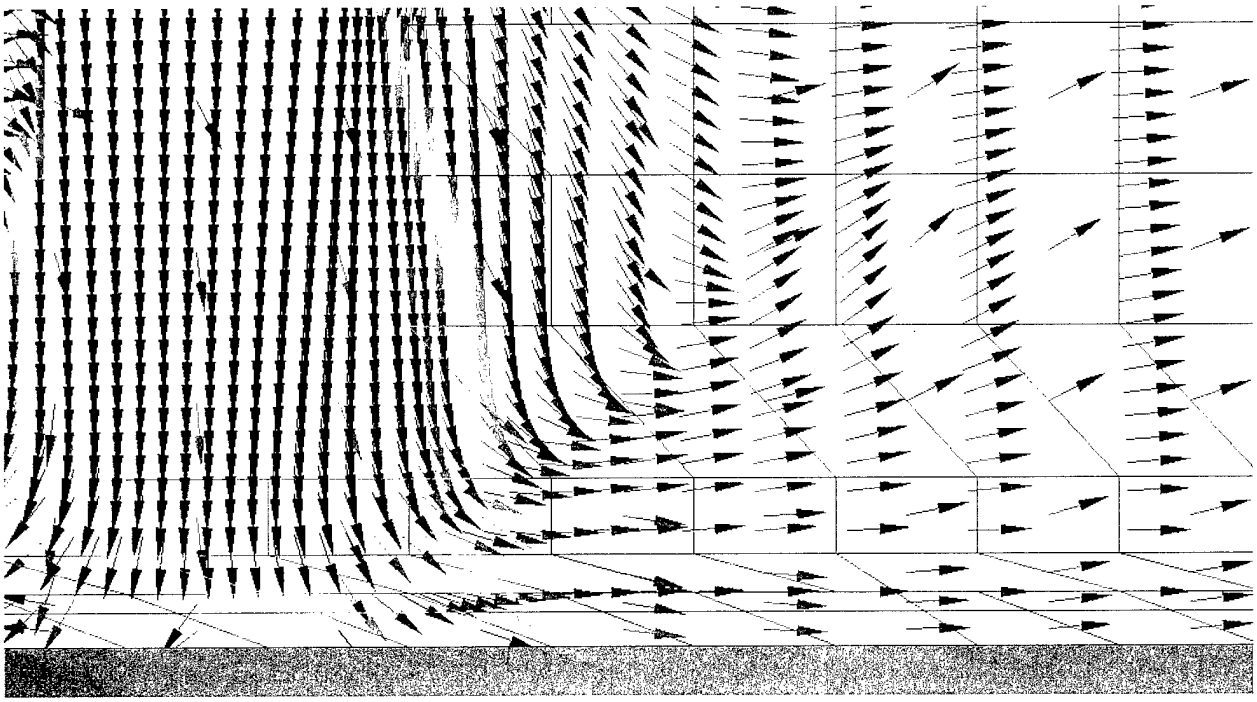

*Figure 5.4. Closeup of Figure 5.1*

## 6. CONCLUSIONS AND RECOMMENDATIONS

The Phase I validation and demonstration work was successfully completed. The suitability and validity of all the computational tools that will be used for efficient and accurate simulation of the turbulent flowfields over entire ship-aircraft configurations has been demonstrated.

The specific conclusions and recommendations from the Phase I work are as follows:

1. The density-based flow solver CFD-FASTRAN is an effective tool for accurate and efficient prediction of VSTOL flow fields. The computational results obtained with CFD-FASTRAN for the in-ground-effect flow fields for the two jet/flat plate validation cases showed good agreement with the experimental data. Plausible and consistent computational results were obtained with CFD-FASTRAN for a complete X-35B aircraft, including open doors, extended gear, and flowing inlets and exhausts. The main features of the flow about the aircraft, including the spreading of the jet and the fountain, were captured.

2. The pressure-based flow solver CFD-ACEU was demonstrated to effectively and accurately handle the near-incompressible flows that occur at the low speeds involved in ship airwake predictions, without the need for Mach Number scaling or pre-conditioning of the system of equations, as would be required in a density-based solver. The computational results obtained with CFD-ACEU with a laminar and LES flow model for the rib in a channel validation case showed good agreement with the experimental results, with the LES model providing the superior comparison especially in separation regions. The results obtained from CFD-ACEU for the flow over a wind-tunnel model of an LHA class ship matched the corresponding wind-tunnel test results with acceptable accuracy.

3. The capabilities of the grid-generation and adaptation package CFD-VisCART were demonstrated for the generation of Cartesian meshes around ships, with a high degree of automation. In particular, it was shown that suitable grids, with appropriate refinement in all regions, could be obtained for ship configurations with a high degree of automation and minimal user intervention.

4. The coupling between the two flow solvers ACEU and FASTRAN using an existing multi-disciplinary computational environment (MDICE) was demonstrated (for the first time in this work), and shown to be effective and efficient. The computational environment uses the chimera-grid approach to couple the flow solutions in different zones or grids, and allows the use of different solvers for different grids. The significance of this work is that it is one of the few instances in which a pressure-based and a density-based solver have been externally coupled in this manner.

The conclusions listed above satisfactorily address all the primary concerns, issues, challenges, and uncertainties regarding the overall methodology to be developed in the Phase II work. In particular, the suitability, fitness, and validation of each of the components to be integrated in the Phase II work (for their respective geometries, flow regimes, and application areas) has been demonstrated, as has the coupling between these components. The overall feasibility of the

technical approach proposed in this work and its ability to satisfy the requirements have therefore largely been demonstrated.

It is therefore recommended to continue the work to the Phase II to integrate the components described above and develop a new simulation environment for prediction of the combined ship airwake VSTOL flow fields.

As explained in Section 4, it was not possible to perform rigorous grid refinement studies within the scope of the Phase I work, for the ship-airwake validations. Such studies are therefore strongly recommended for the Phase I Option work. Such studies would lead to a better understanding of the physical and numerical processes involved in the generation and attenuation of the main vortices, and to a reduction in the discrepancy described in Section 4.2 between the computational predictions and the experimental results for the ship-model airwake.

# 7. OVERVIEW OF PHASE II PLAN

The Phase I work has proven the capability of both the CFD-FASTRAN and the CFD-ACEU codes in predicting the flow fields of VSTOL aircraft and ship airwakes, respectively. The Phase I work also demonstrated the coupling between these two solvers using an existing unstructured chimera technology and the MDICE environment. The Phase II objective is to complete the development of the computational framework, to validate the approach for coupled ship airwake and VSTOL predictions, and to create an efficient effective software package for simulations of the Dynamic Interface.

## 7.1 Conceptual Overview of Proposed Phase II Approach

The conceptual framework is illustrated in Figure 7.1. The SASM module (Ship and Aircraft Simulation Module) depicted in that figure will be developed in the Phase II work, and will play a central role in the overall software package. The individual steps followed in the proposed methodology are as follows:

1. Meshes for the aircraft and ship will be independently generated. Pre-existing meshes may also be used. Any structured or unstructured mesh topology can be used. This provides flexibility in choosing a grid topology most suitable for the geometry and the user and will allow the generation and use of mesh libraries for the aircraft and ships. The Phase I study demonstrated a multi-block structured grid for the aircraft and an adaptive viscous Cartesian grid for the ship.

2. The meshes will be loaded into a Graphical User Interface, or GUI, for convenient specification of initial and boundary conditions and solver parameters. The GUI will also be used to specify the hole cutting surfaces and interpolation parameters for chimera communications.

3. An unstructured chimera module, residing in the SASM environment, will identify cells that should be excluded from the solution process, and determine the lines of communication between the overlapping meshes.

4. An adaptive Cartesian grid module will automatically adapt the ship grid in the overlap region to match the resolution between the two grid systems. This matching resolution is to ensure the accuracy of the coupling.

5. The modified Cartesian ship grid, with its associated boundary conditions and other solver inputs, will be passed to the pressure-based flow solver.

6. The aircraft grid, with its boundary conditions and other solver inputs, will be passed to a density-based flow solver.

7. The solution process of both solvers are initiated from the GUI. As the solution progresses, the necessary solution data is exchanged through the chimera boundaries, ensuring the coupling of the solutions across all the meshes.

8. At specified points in the solution process, solutions files with a common data structure will be generated for use with visualization software, such and CFDRC's CFD-VIEW.

The flow solvers will utilize high order spatial schemes and advance the solution forward in time using a second-order time marching scheme, and a DES or LES turbulence model. A parallel version of the solvers will decrease the run time by distributing the calculations over several computers.

Despite the complexity of the procedure and number of components involved, the process will be controlled easily by the user through a common GUI. The components of the process will be tightly integrated into the SASM computational environment.

Most of the technology needed for this application already exists in the various tools to be used. The proposed Phase II enhancements and further developments of these tools are outlined below.

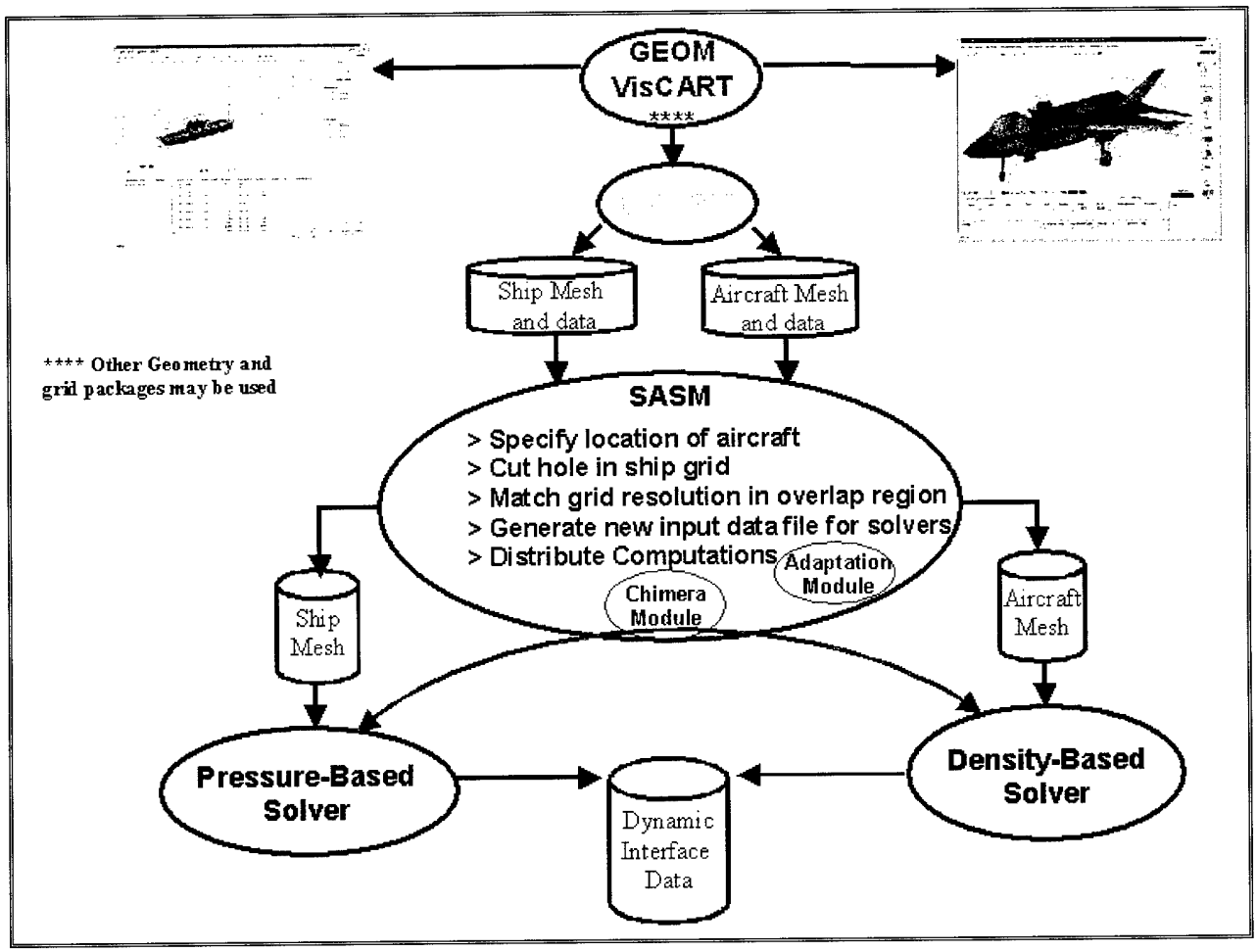


*Figure 7.1. Conceptual Overview of Proposed Computational Environment for Ship and Aircraft Coupled Simulations*

## 7.2 Proposed Development and Software Enhancements

The following additions and enhancements will be made under the Phase II program to enable the proposed coupled ship and VSTOL aircraft calculations.

- Extend an existing unstructured chimera module to support automatic hole cutting and interpolation for arbitrary cell types.
- Develop a Detached Eddy Simulation (DES) model and incorporate it into both the pressure-based and density-based flow solvers. This model will be developed by combining the existing LES and Spalart-Allmaras turbulence models.
- Enhancement of the grid generation capabilities of CFD-VisCART for automatic grid generation and resolution for ship configurations.
- Develop a stand-alone adaptation module, to be optionally used, to refine the ship Cartesian grid to match its cell dimensions with the dimensions of cells of the aircraft grid in the overlap region. This will ensure proper communication across chimera boundaries. This module will be incorporated into the SASM environment.
- Add a second-order time marching scheme to the density-based flow solver.
- Add a time-accurate preconditioner to the density based flow solver.
- Integrate all software components into the SASM environment for efficient and proper data passing and communication.
- Customize the SASM environment for the U.S. Navy's requirements and applications.

### 7.2.1 Unstructured Chimera/Overset Module

Structured overset meshes have been used for many years. However, the extension of the process to a arbitrary polyhedral mesh is a relatively new endeavor. In general, the chimera-overset technology (Refs. 19-20) allows a complex multi-component geometry to be meshed by a number of overlapping meshes. The solution is made continuous across all the meshes by passing the flow information across the mesh boundaries. Conditions at the overlapping mesh boundaries are determined by interpolation from the interior of the neighboring meshes. If points in a mesh lie inside a solid surface, the points are excluded from the solution process, ensuring that there is no flow through the body.

An unstructured chimera module already exists in the MDICE computational environment. This chimera module will be adapted to support arbitrary type grid elements. This will provide great flexibility in mesh construction and problem set up. This approach allows the selection of grid types that best suit the geometries and the local flow conditions. For example, prism grids, stretched tetrahedral grids, or structured grids are well suited for resolution of boundary layers, while Cartesian and tetrahedral meshes are well suited (and easily constructed) for the far field. The hybrid-overset capability will allow the user to obtain ship/aircraft solutions using existing meshes, using newly constructed meshes, or using a combination of old and new meshes.

### 7.2.2 Integrated Adaptive Cartesian Capability

It is proposed that the user have the option to overset any meshes that have been selected for a study into an automatically generated Cartesian mesh. In general, creating a background Cartesian mesh is a simple process. However, for the proposed approach, care must be taken at the overlapping interfaces. Since the ship, aircraft, and background meshes will be generated independently of each other, differences in the local cell dimensions in the overlap regions may be large. If large disparities in the cell dimensions are allowed to remain, excessive truncation errors may be generated in the solution, which will reduce the accuracy of the predictions. In order to eliminate this problem, an adaptation module will be used to refine the Cartesian mesh in the overlap region to better match the cell dimensions in the other meshes. If enabled, this will automatically be invoked from the computational environment immediately after the chimera module has identified the overlap region and the mesh resolution in the aircraft grid in that region.

### 7.2.3 DES Turbulence Model

Studies have shown that Large Eddy Simulations (LES) can accurately model massively separated flows. However, the numbers of mesh points and iterations required often makes the simulation impractical (Ref. 21). On the other hand, RANS turbulence models are widely used for attached boundary layer flows, but are not as accurate in separated regions. Recent papers have proposed a merging of the two simulation methods. The method is referred to as Detached Eddy Simulations or DES. In the DES method of Reference 21, the small eddies in the attached boundary layer region are modeled using a RANS method, while large detached eddies are directly resolved using an LES approach. A DES model may be created from a RANS model by modifying the destruction term for eddy viscosity, d. In a RANS formulation, d is proportional to the distance of the point of interest from the nearest wall. In an LES formulation, eddy viscosity is proportional to a constant multiplied by the grid spacing, D. In a DES formulation,

$$d = \min(d, C_{des}D)$$

where $C_{des}$ is a constant. Therefore, this single model acts as a RANS turbulence model if $d << D$, and as an LES model if $d >> D$.

For Phase II, a Detached Eddy Simulation (DES) capability will be implemented into the CFD-FASTRAN and CFD-ACEU codes. Incorporation of this model will greatly enhance the accuracy of the codes, and is thought to be necessary to obtain the level of accuracy desired.

### 7.2.4 Second Order Accurate Time Marching Scheme

To reduce the risk of damping out important flow features, a higher order time integration will be added to both the structured and polyhedral unstructured flow solver modules in CFD-FASTRAN. The most likely selection will be the Implicit Trapezoidal scheme, which is often referred to as the Crank-Nicholson (C-N) Method. The C-N Method is considered to be unconditionally stable and provides second order accuracy in time. Incorporation of this model will enhance the accuracy of the CFD-FASTRAN code in predicting ship airwakes and the VSTOL flow field.

### 7.2.5 Time-Accurate Pre-conditioner

Obtaining solutions using characteristic-based schemes for the compressible Euler and Navier-Stokes Equations become increasingly problematic with decreasing freestream Mach Number and/or with an increasing disparity between the lowest and highest velocities appearing in the flow field. There are two main reasons for the difficulty (Refs. 22-25). The first is a reduction in accuracy because of the numerical coupling between the pressure and the velocity fields in the momentum equation. The second reason is a reduction in the efficiency of the scheme because of the stiffness of the system's eigenvalues. Several methods of addressing the problems have been documented. Currently, the approach of Reference 24 is thought to be the most appropriate for the CFD-FASTRAN solver. In this approach, the time-derivative term of the Navier-Stokes Equations is multiplied by a conditioning matrix that rescales the eigenvalues of the entire system. An attractive alternative to Reference 24 is to use a dual time-stepping approach in which a term consisting of a derivative with respect to "pseudo-time" is added to the time-dependent Navier-Stokes Equations (Ref. 25). This term is iteratively converged in the pseudo-time variable to give the time-accurate update to the original system. In either case, the addition of the preconditioner will provide the accuracy and efficiency needed for the low-speed ship airwake simulations.

### 7.2.6 Software Tools Integration and Customization

The various computational tools will be tightly and efficiently integrated to provide an easy-to-use computational framework. The coupling between the density-based and pressure-based flow solvers will be seemless to the user and will be completely handled by the SASM environment. CFD-FASTRAN and CFD-ACEU already have all the necessary software coding for such external coupling, as demonstrated in this project. The unstructured chimera module is an MDICE module and is already fully integrated into the environment. This capability was already demonstrated in Phase I for a generic aircraft and ship configuration. The adaptation module will also be fully integrated into the environment. A common graphical user interface (or panels) will be developed to manage and control all operations in the environment, as outlined in Figure 7.1.

The GUI will incorporate tools for the following tasks:

- Loading the ship and aircraft grids
- Positioning the ship on aircraft (provide $d_x$, $d_y$, $d_z$)
- Performing chimera hole cutting
- Adapting the grid in the overlap region (Optional)
- Creating the new ship and aircraft grid and data files
- Performing domain decomposition for parallel processing
- Specification of the node distribution for parallel processing
- Launching the solvers for the computations
- Launching the CFD analysis tool for solution monitoring and analysis

This GUI or panels will be created using the common CFDRC FOX libraries.

The proposed Phase II work plan will provide a highly flexible computational framework for coupled ship and VSTOL aircraft simulations. The framework will satisfy the objective of this work by enabling quick and efficient generation of flow databases to be used in the development of a Dynamic Interface database. The use of both pressure-based and density-based flow solvers, and the use of separate arbitrary topology grid systems for the ship and aircraft will allow the user to examine any flow speed at any WOD conditions with relative ease.

## 8. REFERENCES


1. Polsky, S.A. and Bruner, C.W.S., "Time Accurate Computational Simulations of an LHA Ship Airwake",AIAA-2000-4126, August 2000.
2. Tai, T.C. and Cario, D., "Simulation of DD-963 Ship Airwake by Navier-Stokes Method", AIAA-93-3002.
3. Tai, T.C. "Simulation and Analysis of LHD Ship Airwake by Navier-Stokes Methods", Presented at the NATO RTO Symposium on Fluid Dynamics, Netherlands, Oct. 1998.
4. Liu, J. and Long, L.N., "Higher Order Accurate Ship Airwake Predictions for the Helicopter/Ship Interface Problem", Presented at the American Helicopter Society, Annua Forum, Washington D.C., May 20-22, 1998.
5. Tattersall, P., Albone, C.M., Soliman, M.M., and Allen, C.B., "Prediction of Ship Airwakes over Flight Decks using CFD", A report to the Department of Aerospace Engineering, University of Bristol, UK.
6. Anupam, S. and Long, L.N., "High Order Accurate Solutions of Ship Airwake Flow Field Using Parallel Computers", Department of Aerospace Engineering, Pennsylvania State University.
7. Squires, K.D., et al., "Progress on Detached-Eddy Simulation of Massively Separated Flows", AIAA-2002-1021, January 2002.
8. CFD Research Corporation, CFD-FASTRAN User's Manual, Theory Manual, 2002.
9. CFD Research Corporation, CFD-ACEU User's Manual, 2002.
10. Smagorinsky, J., "General Circulation Experiment With the Primitive Equations. I. The Basic Experiment," *Monthly Weather Review*, **91**, pp. 99-164, 1963.
11. Germano, M., Piomelli, U., Moin, P. and Cabot, W.H., "A Dynamic Subgrid-Scale Eddy Viscosity Model," *Physics of Fluids A*, **3**, pp. 1760-1765, 1991.
12. Menon, S.M., Stone, C. Sankaran, V. and Sekar, B., "Large Eddy Simulations of Combustion in Gas Turbine Combustors," AIAA 2000-0960, 38th AIAA Aerospace Sciences Meeting & Exhibit, Reno, NV, January 10-13, 2000
13. CFD Research Corporation, CFD-GEOM User's Manual, 2002.
14. CFD Research Corporation, CFD-VisCART User's Manual, 2002.
15. Herman Schlichting, Boundary Layer Theory, McGraw-Hill Book Company, 1979.
16. Kuhn, R.E., et al. "On the Anomalies in Single-Jet Hover Suckdown Data", NASA-TM-102261, August 1991.
17. Wardwell, D.A., et al. "Jet-Induced Ground Effects on a Parametric Flat-Plate Model in Hover." NASA-TM-104001, March 1993.
18. Werner, H. and Wengle, H. "Large Eddy Simulation of Turbulent Flow Over a Square Rib in a Channel," Advances in Turbulence 2, pp. 418-423, 1989.
19. Benek, J.A., Dougherty, T.L., and Buning, P.G., "Chimera: A Grid Embedding Technique", AEDC-TR-85-64 (AD-A167466), April 1986.
20. Rock, S.G. and Habchi, S.D., "Validation of an Automated Chimera Methodology for Aircraft Escape Systems Analysis", AIAA-98-0767, January 1998.
21. Spalart, P.R. et al., "Comments on the Feasibility of LES for Wings, and on a Hybrid RANS/LES Approach", 1st AFOSR International Conference on DNS/LES, August 4-8, 1997, Ruston, LA.

22. Turkel, E. "Preconditioned Methods for Solving the Incompressible and Low Speed Compressible Equations," Journal of Computational Physics, Volume 72, pp. 277-298, 1987.
23. Merkle, C.L. and Choi, Y.H., "Computation of Low Speed Flow with Heat Addition," AIAA Journal, Volume 25, p. 831, 1987.
24. Choi, Y.H. and Merkle, C.L., "The Application of Preconditioning in Viscous Flows," Journal of Computational Physics, Volume 105, pp. 203-223, 1993.
25. Shuen, J.S., Chen, K.H., and Choi, Y.H., "A Time-Accurate Algorithm for Chemical Non-Equilibrium Viscous Flows at All Speeds," AIAA-92-3639, 1992.